In response to Alan Frieds comments from October the 16th, 2018.

This is an excellent paper representing very careful and well thought out procedures and analysis methods. The paper is very well written and the results are very sound. I particularly like the fact that two different precision regimes have been identified (within the PBL and above the PBL) and yield different results due to differences in alignment caused by aircraft vibrations. We often see this effect in our measurements and highlighting them here is a further illustration of the care devoted to the measurements presented. The one thing that should be added is a brief section indicating how the in-flight precisions were determined. Did the authors base this on the precision of zero air measurements or the precision of ambient measurements under stable conditions? In the case of the latter, ambient variability cannot be ruled out the in-flight precisions may be even better than indicated. I recommend final publication after the following minor points are addressed. As you can see, these are all very minor and serve to clarify some of the discussion.

Dear Alan,
Thank you very much for your kind and helpful comments on the procedures and analysis methods presented herein. The in-flight precisions are in fact based on ambient measurements at stable conditions. Ambient variability can thus not be completely ruled out, however in-flight precision figures could only benefit from sampling gas from pressure cylinders. We further completely agree, that a pressure-stabilized enclosure would be the ultimate solution. This would imply heavy modifications on the instrument and render our acquired FAA certification (required for all European Research Aircraft) invalid. For this reason it has not yet been done at this point.

1. **Introduction, Line 6: change the word "remain" to "have"**
   The wording has been changed to:
   "[...] is a strong greenhouse gas and is expected to have the most important ozone-depleting anthropogenic impact throughout [...]"

2. **Introduction, Line 16: Since there have been extensive measurements of atmospheric gases well before QCLs and ICLs in the mid-IR using for example, liquid nitrogen cooled lead-salt diode lasers as well as other sources, a brief sentence giving a reference to some of this work should be included. One can cite numerous sources, but one convenient way (at the risk of being self-serving) would be to cite our text book chapter which has many of these references (Chapter 2: Infrared Absorption Spectroscopy by A. Fried and D. Richter, in the book Analytical Techniques for Atmospheric Measurement, edited by D.E. Heard, Blackwell Publishing, 2006).**
   A brief sentence giving a reference to some of this work has been added:
   "[...] Spectroscopic instruments making use of molecular ro-vibrational absorption allow for high temporal coverage through fast instrument response times (Chen et al., 2010). Some have already been used for airborne research, e.g. established IR spectrometers (O'Shea et al. (2013); Santoni et al. (2014); Cambaliza MOL (2015); Filges et al. (2015)). Significant effort led to instruments operating in the mid infrared (IR) region, e.g. liquid nitrogen cooled lead-salt diode laser based spectrometers (Fried and Richter, 2007). With the commercial availability of continuous-wave lasers emitting in the mid IR region near ambient temperature (Capasso (2010); Vurgaftman et al. (2015); Kim et al. (2015), Beck et al. (2002)) several new instrument designs have emerged (McManus et al. (2015); Zellweger et al. (2016)). [...]"

3. **Introduction, Line 20: Please change the wording "custom-built QCL..." to "custom-built difference frequency generation (DFG) absorption spectrometer"**
   The relevant sentence has been changed to:
   "[...] reported on a custom-built difference frequency generation (DFG) absorption spectrometer [...]"

4. **Introduction, Line 27: Are you strictly referring to established cavity ring-down instruments here or are you referring to more generally IR absorption instruments? Since you mention the "described spectrometer", I think you should change "established cavity ring down" to "established IR spectrometers"**
   We are referring to established IR spectrometers in general. The wording has been changed accordingly to:
   "[...] used for airborne research, e.g. established IR spectrometers [...]"

5. **Page 4, Line 25: It would be useful to the reader to further elaborate on the meaning of "jeopardized nominal system startup". Do you simply mean the large in rush current to get the pump going is more than the airplane circuit breakers can take, or does this mean that this may cause damage to other parts of the instrument?**
Inrush currents have previously been too large, causing circuit breakers to trigger. Depending on whether computer/data analysis systems sharing the same circuit breaker, were already turned on, sudden power loss has previously implied further consequences. However, the few power loss situations we have experienced with this instrument have had no noticeable effect. The following sentence has been added for clarification:
"[...] nominal system startup (priv. comm. Stefan Müller, MPI Mainz). Sudden power failure, due to over-current triggering aircraft circuit breakers, may lead to failures in the data analysis equipment. [...]"

6. **Figure 5: It would be very helpful to the reader to indicate the mixing ratios in the figure caption used in recording the various spectra.**
The mixing ratios will be indicated for each species in the three microwindows in a revised version of this manuscript.

7. **Page 10, Line 2: Where is the weak CH4 line relative to the C2H6 line which is used for spectral shifting of the C2H6 feature?**
In a revised version of this manuscript line 1/2 on Pg. 10 has been changed to: "A single adjacent CH_4 line, located at $2989.981\,cm^{-1}$ has been included in order to obtain good C_2H_6 data even under these challenging conditions."

8. **Page 11: This is a very nice discussion of the various broadening parameters and how they are handled. However, this reviewer wonders how important actually including the self-broadening and water broadening are in the final fits since these are smaller by the fact the sampling pressure is 50-mb and the overall spectral stability is in the $10^{-3}cm^{-}1$ range? The air broadening at this pressure is only $\sim 0.0035cm^{-}1$ which is close to the spectral stability. Perhaps a brief mention of how the inclusion of self and water broadening changes the retrieved results should be included.**
Not including the self and water foreign broadening leads to relative errors in the range of 0-2%, depending on the species of interest. While small for C_2H_6 and CH_4 with $< 0.03\%$, the influence on retrieved CO is rather large with $\sim 2\%$.
"[...] Not including the self and water foreign broadening leads to relative errors in the range of 0-2% for the described setup, depending on the species of interest. While small for C_2H_6 and CH_4 with $< 0.03\%$, the influence on retrieved CO is rather large with $\sim 2\%$. [...]"

9. **Figure 7 and Its Caption along with Page 13, Line 1: At the FLAIR (Field Laser Applications in Industry and Research) the Program Committee strongly recommended that references to "Allan Variances" should be denoted "Allan-Werle Variances" in honor of the late Peter Werle who adapted this concept to atmospheric measurements. Below I include a portion of the Program Committee's Obituary for Peter Werle and its recommendation (this need not be included in the final paper but is included here for your reference). Also, what mixing ratios were used in recording Fig. 7 (zero air or calibrated standard mixing ratios)?**
Thank you very much for pointing this out. Occurrences of "Allan variance" have been changed accordingly in a revised version of this manuscript.

10. **Page 15, Discussion of Fig. 10: In comparing flask and in situ measurements it should be mentioned that care must be exercised in that during times of rapidly changing ambient mixing ratios one may not get agreement between the slow flask samples and fast in situ measurements. Although this is obvious, it is worth mentioning here. I see this is discussed in the Fig. caption 13 but it is also worth mentioning here.**
The following short sentence has been added to the manuscript:
"[...] both sampled through an upstream dryer. It should be noted, that care must be taken when interpreting the differences between slow flask samples and fast in situ measurements for high-variability flight segments. [...]"

11. **Page 18, in the discussions of cabin pressure dependence: The authors should mention that it is not possible to accurately compare the dependence of one instrument relative to another since many instrument-dependent**

and other factors come into play. For example, some of the dependence is due to the changing mixing ratios for the species under study in the open-air path. Additional dependencies result from movement of optical windows and other components and are instrument dependent. Also, we find that the rate of cabin pressure change is an important factor, and this is specific to the particular aircraft and the flight pattern employed. Hence, the left side of Fig. 12 may not tell the whole story. We find that the delta Pcabin/delta time comes into play between zero acquisitions, and I would expect the same thing here. Perhaps a comment on this should be mentioned.

The relevant text portion has been rephrased to:

"[...] A severe cabin pressure dependence in excess of $0.3 ppb hPa^{-1}$ in CH_4 mixing ratio has been previously reported for airborne TILDAS instrumentation (Pitt et al., 2016). This instrumentation however physically differs from the one reported here. It is not possible to accurately compare the dependencies of one instrument relative to another since many factors/quantities involved are instrument-specific, e.g. the open-path length, the positioning and properties of optical elements, like windows and mirrors, the stiffness and thermal expansion coefficients of employed optical stands, etc.. We were nevertheless able to effectively minimize cabin pressure dependencies during operation of the QCLS instrument aboard the C130 using the calibration strategy from Sect. 2.3. [...]"

In response to Anonymous Referee #2 comments from November the 9th, 2018.

This paper describes the performances of an analyser of the major greenhouse gases in air on board of an aircraft. Details are provided on the analyser hardware, the analytical software and the calibration method, followed by an evaluation of the performances by comparison with other analysers present during the same flight. While the analyser itself is not new and was already described in a previous paper (McManus 2011), in this work the number of analysed compounds was extended, the in situ performances were looked at more deeply, and the calibration method was improved. The paper is generally well written, well-structured, clear, and provides lots of details on the instruments and methods. However the section on performance evaluation needs some more work, both in its content and format. I therefore recommend a minor revision before the paper can be published in AMT.

Comments on the terminology
- Units to be written in plain (not italic) format - The format to display a value with its unit is "value-space-unit" for example "204m" on page 4 should be written "204 m"
- "mixing ratio" to be replaced by "amount fraction", expressed in mol mol-1 (nmol mol-1 for ppb, µmol mol-1 for ppm).
- Names of molecules to be written in plain (not italic) format.
- Allan deviation seems to be confused with Allan variance. When values are reported in the same unit as the concentrations, this should be a deviation. Please check the correct usage over the document

Dear Referee,
Thank you very much for the detailed and very helpful comments and for the time spent on reading and reviewing this manuscript. We greatly appreciate it. The comments made on terminology were of great help and have been implemented in a revised version of the manuscript. We will directly follow up on the specific comments.

Specific comments by section:

1. **Section 2.1: the text describes two sealed cells containing CH4 and N2O. Where are they on Figure 1? Please indicate the purity of the gas and its pressure.**
   There is only a single sealed cell containing CH_4 and N_2O. Its position has been marked in a revised version of Fig. 1. The gas inside the cell has an approximate pressure of 3500 Pa. The gas does not need to be pure. As the laser scans over the absorption features of CH_4 and N_2O the laser can be spectrally referenced to the relevant molecular absorption lines, which is the single purpose of the sealed cell.

2. **Section 2.3: please provide more information on the calibration mixtures. In particular NOAA standards are all identified within NOAA database and you could just provide their reference to allow the users looking at all values measured by NOAA. At least please indicate the nominal amount fractions, their uncertainties, and the isotopic composition for CO2. This last value is of importance as you noticed a bias between the CO2 amount fractions measured with your instrument and those measured by the PICARRO.**
   We included the requested details on the used NOAA standards for CH4 and CO2. However, we have to note, that we used working standards of synthetic nature from *Air Liquide* due to the large amount of needed calibration gas. Usually these are produced with CO_2 from natural gas & oil combustion processes. We determined the CH_4 and CO_2 values of each working standard gas cylinder using a Picarro G-1301m. This has the drawback that we do not know the isotopic composition of our working standards. The reason why we did not send our working standards to a central lab is because the influence of the isotopic composition had been considered negligible at this stage (Chen et al., 2010). It was only in late summer 2018, that we found out (during development of JFIT) that the instrument was using a $^{13}C^{16}O_2$ line to derive ambient CO_2. We assume the large bias originating from differences in isotopic composition in our working standards relative to the natural terrestrial abundances.
   "[...] The cylinders have been cross-calibrated against NOAA standards and are thus traceable to World Meteorological Organization (WMO) standards for CH_4 (Cert.-Nr. CB11361, WMO X2004A for CH_4 (Dlugokencky et al., 2005)) [...]"

"[...] In this study we used working standards of synthetic nature from *Air Liquide*. Usually these are produced with CO_2 from natural gas & oil combustion processes. We determined the CH_4 and CO_2 values of each working standard gas cylinder using a NOAA-anchored (Cert.-Nr. CB11361) Picarro G-1301m. This has the drawback that we do not know the isotopic composition of our working standards as its impact had been considered negligible, e.g. (Chen et al., 2010). We only found out during development of JFIT, that the instrument is using a $^{13}C^{16}O_2$ line to derive ambient CO_2. We estimate the required isotopic composition of such a CO_2 to be 98.447% primary isotopologue and 1.079% secondary isotopologue or $\delta^{13}C = -19.6\,‰$ which seems reasonable according to B. Coplen et al. (2002). Since we are reporting retrieved mole fractions relative to the WMO scale, only the working standard reproducibility contributes to the total uncertainty of CH_4. Uncertainty on CO_2 is difficult to assess here because of the unknown isotopic composition in our working standards. [...]"

3. **Section 4, ground-based performance: the reported Allan deviations seem a bit large. Compared to McManus 2011 on CO 2 for example, a factor 10 is noted. Please consider revising the statement that "values are in good agreement with the values reported by Aerodyne" and/or provides further support. Is there an effect of the calibration system described in 2.3, which is said to be used to check the stability and the linearity?**
The lasers frequency reported in McManus 2011 differs from the emitted frequency reported in this publication. Therefore it is not possible to directly compare with the values reported in McManus 2011. Here we are referring to the specifications reported by Aerodyne Inc. for this particular instrument. Nevertheless we removed this sentence as it is not necessary at this point. Although the calibration system has a strong influence on the instruments accuracy, we see no variation in precision after carefully looking at signal changes before and after calibration versus similar intervals between calibrations.

4. **Section 5: while the traceability of measurements with the QCL is clear (calibration with NOAA standards), nothing is indicated regarding the PICARRO. This is needed to fully understand the origin of biases. It seems that an anchored to NOAA is assumed, but this deserves further details (which standards? How many calibration steps? Isotopic composition?). When both instruments are compared, it would be more useful to express the difference in amount fraction, both in the text and in the graphs. This should then be compared with their uncertainties, not taking into account common sources of uncertainties such as NOAA uncertainty if all amount fractions are expressed on the same scale. Going beyond this, some consideration on how this compares with the Data Quality Objectives set by WMO would be of interest. The treatment of the constant bias found between the AERODYNE and the PICARRO analysers needs to be improved. Are both analysers calibrated directly with NOAA standards? How different are the calibration gases? It would be valuable to estimate the bias one could expect from the isotopic difference, as done for example in the paper of Chen et al. (Atmos. Meas. Tech., 3, 375–386, 2010), and compare with the observed bias. Indeed, an observed bias of 10 µmol mol -1 seems very large.**
The PICARRO instrument is anchored to NOAA. CO2 is WMO X2007, CH4 is WMO X2004A, CO is WMO X2014A. It is calibrated hourly during flights using a fixed standard and weekly using a three-point calibration with high, low and target calibration standards. The corresponding references have been implemented in a revised version of the manuscript. Concerning the second part of this comment: it is important to know the dynamic range that is covered when looking at differences between instruments. Vanishing differences at vanishing dynamic range do not tell the whole story about instrument performance. We included both, the differences (as histograms in Fig. 13) and the absolute values (dynamic range) in Fig. 10 and 11. The origin of the biases is not yet fully understood. It was suggested that water vapor correction could have an impact on this. The reason for this assumption is that the calibration standards are always dry, whereas sampled air is not dried before entering the sample cell. Correlation plots however show no signficant influence of water vapor on the residuals between the dry-air-sampling Picarro and the QCLS. It is therefore very unlikely that the water vapor correction is the source of the large bias in CO_2. Instead we identified the difference in isotopic composition of the calibration standard versus sampled atmospheric air as the most probable cause. Chen et al. (Atmos. Meas. Tech., 3, 375–386, 2010) estimated the influence for a Picarro greenhouse gas analyzer measuring the primary CO_2 isotopologue. It is commonly assumed that the influence of isotopic composition is on the order of 0.1 ppm. Using the $^{13}C^{16}O_2$ line at $2227.604\ cm^{-1}$ via HITRAN-based direct absorption spectroscopy, we estimate a much larger influence, that could well explain the bias encountered (see above). We estimated the required isotopic composition of such a CO_2 to be 98.447%

primary isotopologue and 1.079% secondary isotopologue ($^{13}C^{16}O_2$). We included this in the text. It is therefore one of the major findings of this study, that knowledge on isotopic composition of the calibration standards is of paramount importance when using the mentioned absorption line.

"[...] In situ CH_4, CO_2, and CO were measured using a PICARRO G2401-m cavity ring-down spectrometer, and in situ CO_2, CH_4, and $H_2O(g)$ were measured using a PICARRO G2301-m cavity ring-down analyzer. Both PICARRO instruments are anchored to WMO X2007 for CO_2 (Zhao and Tans, 2006), WMO X2004A for CH_4 (Dlugokencky et al., 2005) and WMO X2014A for CO (Baer et al., 2002). [...]"

"[...] In this study we used working standards of synthetic nature from *Air Liquide*. Usually these are produced with CO_2 from natural gas & oil combustion processes. We determined the CH_4 and CO_2 values of each working standard gas cylinder using a NOAA-anchored (Cert.-Nr. CB11361) Picarro G-1301m. This has the drawback that we do not know the isotopic composition of our working standards as its impact had been considered negligible, e.g. (Chen et al., 2010). We only found out during development of JFIT, that the instrument is using a $^{13}C^{16}O_2$ line to derive ambient CO_2. We estimate the required isotopic composition of such a CO_2 to be 98.447% primary isotopologue and 1.079% secondary isotopologue or $\delta^{13}C = -19.6\,‰$ which seems reasonable according to B. Coplen et al. (2002). Since we are reporting retrieved mole fractions relative to the WMO scale, only the working standard reproducibility contributes to the total uncertainty of CH_4. Uncertainty on CO_2 is difficult to assess here because of the unknown isotopic composition in our working standards. [...]"

5. **Section 5, uncertainties: it is not so common to see combined uncertainties considered in such measurements, and the effort of the authors is certainly valuable. However some consideration on how these values compare with other instruments would be required. Is the calibration procedure specific to this instrument? Does this imply a larger uncertainty than for others? Would you say this instrument has comparable precisions than others?**
The calibration procedure described herein is not instrument specific. It could be applied to other in situ instruments as well. Regarding the accuracy involved, there is always a trade-off between measurement time and accuracy: Increasing the number of calibration cycles improves achievable accuracy at the cost of observation time. It does not imply a larger uncertainty than others, as we do not use the online calibration mixing with the MFCs when taking data (Online mixing would add the uncertainty on the mass flow controllers on top). The instrument described herein is unique in that it offers many simultaneously observed species. It may be possible to find instruments showing better precision figures measuring a single or two species but we seriously doubt, that any other instrument with those many species sampled simultaneously will show better precision figures. Furthermore, as described in the text we estimate the uncertainty on calibration sequence evaluation with 2σ, which is again a worst-case assumption. Unfortunately we had a numerical error in the first version of the manuscript and the values listed in Tab. 3 were not double the precision. We corrected this in the revised version of the manuscript. We further included a short sentence on precision comparison with the available PICARRO instrument:
"[...] Precision (uncertainty) figures given in Tab. 3 can be compared to 2s-1σ PICARRO G2401-m airborne precision (uncertainty) estimates based on ambient measurements at stable conditions of 0.3 (2) ppb, 0.02 (0.1) ppm and 2.0 (5) ppb for CH_4, CO_2 and CO, respectively. [...]"

6. **Section 5, discussion on instruments precisions: Allan deviations (not variance) were measured before the flight and during the flight. It is not very clear how those values compare. One would expect the lowest values during ground-based measurements, presumably recorded on gas mixtures with constant flow rate and pressure. During the flight, other sources of instabilities can increase the noise of the instrument. However some of the values appear to be lower during the flight (above the planetary boundary layer only). This would need some further explanation.**
Allan variances were not measured during flights. The in-flight precision values are instead based on ambient measurements at stable conditions. Ambient variability can thus not be completely ruled out. Meaning, we are looking at the worst case scenario here. Thank you for pointing us towards this mistake on the ground-based precision values. The values reported for ground based operation were based on an older version of the retrieval software. We have corrected this in a revised version of the manuscript.
"[...] Typical in-flight precision figures based on ambient measurements at stable conditions for both regimes [...]"

7. **Conclusions: the advantages and drawbacks of the aerodyne instrument could be better highlighted. The large number of species analysed together is certainly an interesting feature, but it seems to come with increased noise compared to CRDS analysers. Is that really the case or is this a wrong impression coming from an increased in-flight noise which could impact other analysers as well?**
Here, we do not want to compare the two instruments against each other. Instead our goal is to demonstrate the suitability of the described instrument, given the calibration approach and post-processing described herein, for airborne observation with the ultimate goal of inferring local to regional fluxes. The instrument has advantages and drawbacks when directly compared to CRDS analyzers. One of the drawbacks is the reduced absorption path length and the resulting lower precision, aswell as the large amount of calibration gas necessary for 10 % of the measurement time. A big advantage is the simultaneous measurement of all targeted species. There is practically no dead time in between measurements, which is especially useful in close vicinity to sources and/or for young weakly dispersed (spatially narrow) plumes. This instrument sees everything, while there is a certain chance with sequentially probing instruments of missing a narrow plume or not getting the peaks right. This is further described in Sect. 5. The large number of observed species is another big advantage that can be used for source attribution.

Line-by-line comments:

1. **Page 3, Line 5: you may clarify that "DLR" in the title is the name of the laboratory owning the spectrometer.**
The relevant sentence has been changed to include a definition of DLR:
"[...] The spectrometer system used here builds upon the *Dual Laser Trace Gas Monitor*, a commercial tunable IR laser diode absorption spectrometer (TILDAS) available from *AERODYNE RESEARCH INC., Billerica, USA*, acquired by *Deutsches Zentrum für Luft- und Raumfahrt* (DLR) in late 2016. [...]"

2. **Page 4, Line 25: you may keep SLPM for the flow rate, but indicate the value in mL min-1 as well**
We don't really see the benefit of reporting flow rates in mL min-1, but 23 SLPM would yield 23000 mL/min at standard conditions ($p = 101325\,\mathrm{Pa}$, $T = 273.15\,\mathrm{K}$). We thought about converting SLPM to SI units $1\,\mathrm{SLPM} = 1.68875 \frac{\mathrm{Pa\,m^3}}{\mathrm{s}}$ but we omitted this, because we assumed SLPM to be a commonly used unit for in situ measurements.

3. **Page 5, Line 19: why the use of "cross-calibrated" rather than "calibrated"? Does it involve a particular method?**
Here, we want to express the fact, that we calibrate our working standards using a Picarro G1301-m to NOAA standards as described above. This is what we refer to with "cross-calibration".

4. **Page 5, Line 32: the entire sentence may be rewritten to express more clearly that no dilution was introduced at this stage, which is why you do not need to take into account an uncertainty on the flow rate measurements.**
The relevant text portion has been rephrased to:
"[...] The online mixing feature is not used for in-flight calibration. Hence, no dilution of the calibration standard with zero air is introduced during flights and the uncertainty on the flow rate measurements can be omitted. Online mixing (relevant for linearity checks) adds the uncertainty of the controlled mass flow on top of the gas cylinder uncertainties. [...]"

5. **Page 10, Line 14-15: what is meant by "not accurately constrained"? There is certainly an issue with the difference in isotopic composition between the sample and the calibration gas, and this aspect deserves a better treatment in the paper. However at this point you are describing the fit of the spectra, and the statement about constraining the isotopic composition of the sample is unclear. Does this mean constraining the fit? The fit window?**
We agree that this information is not needed at this point for describing the spectral fit. It is dealt with in Section 5. We thus removed the complete sentence.

6. **Page 12, Line 14 "excluding absolute error". Do you mean uncalibrated or expressing the precision only? Line 15: "values reported by Aerodyne". Which paper? McManus 2011?**

Here, we state the 1-sigma precision and measurement frequency only. The absolute error stated by the pressure transducers manufacturer is stated with ± 0.5 hPa. The relevant text portion has been rephrased to:
"[...] The volumetric flow rate stabilized at 23 SLPM for a sample cell pressure regulated at 50.0 ± 0.5 hPa (0.2 hPa precision @ 5 Hz). [...]"

7. **Page 18, Line 2-3: "we were not able to reproduce..." seems a rather negative introduction for a positive result, as everything was made to be insensitive to the cabin pressure. Consider rephrasing.**
The relevant text portion has been rephrased to:
"[...] A severe cabin pressure dependence in excess of $0.3 ppb hPa^{-1}$ in CH_4 mixing ratio has been previously reported for airborne TILDAS instrumentation (Pitt et al., 2016). This instrumentation however physically differs from the one reported here. It is not possible to accurately compare the dependencies of one instrument relative to another since many factors/quantities involved are instrument-specific, e.g. the open-path length, the positioning and properties of optical elements, like windows and mirrors, the stiffness and thermal expansion coefficients of employed optical stands, etc.. We were nevertheless able to effectively minimize cabin pressure dependencies during operation of the QCLS instrument aboard the C130 using the calibration strategy from Sect. 2.3. [...]"

Comments on figures:

1. **Figure 7 it is not clear if the amount fractions are provided after calibration or not. The legend seems to indicate calibrated values, but the y-axis in the right plot indicates "Methane RAW [ppt]" which would mean raw values before calibration. Please clarify.**
The depicted methane amount fractions are indeed raw signals before calibration. A synthetic calibration gas has been mixed from zero and calibration gases using the described calibration system, in order to verify the linearity of retrieved amount fractions.

2. **Figures 10 and 11: it is too uneasy to compare both analysers on the plots. Differences would be more interesting, as the paper does not include any consideration on the amount fractions of the gases.**
It is important to know the dynamic range that is covered when looking at differences between instruments. Vanishing differences at vanishing dynamic range do not tell the whole story about instrument performance. We included both, the differences (as histograms in Fig. 13) and the absolute values (dynamic range) in Fig. 10 and 11.

3. **Figure 12: y-axis of the right plot is the methane amount fraction. Use a symbol and unit such as "xCH4 / (nmol mol-1)" and indicate in the legend "xCH4 is the methane amount fraction".**
xCh4 is commonly used for total column measurements. We therefore refrain from changing the axis label here.

In response to Anonymous Referee #4 comments from October the 30th, 2018.

The paper by Kostinek et al. presents ground-based and in-flight performance assessments of a commercial trace gas analyzer (TILDAS, Aerodyne Research Inc.) after its adaptation for airborne operation. The subject is highly topical and targets a key issue that every scientist is facing when taking decision on analyzer selection. This can even be critical considering the stringent place and measurement-time limitations of flight campaigns. Here, the author's choice is on a dual-laser direct absorption spectrometer with multi-species (i.e., five compounds) detection capabilities deploying state-of-the-art mid-IR laser sources (both QCL and ICL). The in-flight intercomparison with CRDS-based instruments and flask samples is an important element of the manuscript that can be of interest for the community involved in airborne measurements. The manuscript is well written, and I recommend publication after addressing some comments and changes listed below.

Dear Referee,
Thank you very much for your careful review and the detailed, helpful comments. We greatly appreciate all your work involved with reviewing this manuscript. The comments include very interesting thoughts and insights. Especially those on instrument details sparked some new ideas to further improve the instrument performance in the future. The technical level of the specific comments is quite high. We hope to have answered to your full expectation.

General comments:

1. **The title should better reflect the content of the manuscript. Given that for the measurements the spectrometer is equally using both QCL and ICL devices, this should be weighted the same. Furthermore, the instrument was mainly adopted and not modified for airborne operation. Thus, my suggestion is to write: "Adaptation and performance assessment of a dual-laser mid-IR direct absorption spectrometer for ..."**
   We agree, that the title should weigh QCL and ICL the same, we thus modified the title to include both after the "initial decision" phase. Based on your suggestion from above we further changed the title to "Adaptation and performance assessment of a Quantum / Interband Cascade Laser Spectrometer for simultaneous airborne in situ observation of CH4, C2H6, CO2, CO and N2O"

2. **The abstract should focus on summarizing briefly the highlights and findings of the presented work. Thus, I suggest starting directly with L7, "Here we demonstrate..."**
   We modified the abstract based on this comment:
   "Tunable laser direct absorption spectroscopy is a widely used technique for in situ sensing of atmospheric composition. Aircraft deployment however, poses a challenging operating environment for instruments sensing climatologically-relevant gases in the Earth's atmosphere. Here, we demonstrate the successful adaption of a [...]"

3. **Although the introduction contains a brief hint about the large number of available measurement techniques for airborne atmospheric measurements, it is unfortunate that the authors completely refrain to motivate their choice for a particular analyzer. Clearly there are some benefits of having multi-species capabilities at slightly higher sampling rate, but how this compensates for the obvious limitations, such as cabin pressure dependence, frequent high-flow calibration requirements, tedious post-processing of the raw spectral data, high power and calibration gas consumption, etc.? A more elaborate discussion on advantages/disadvantages of the chosen approach would significantly improve the manuscript.**
   We have added a brief statement in the introduction on the motivation for the particular analyzer used. As stated in the response to reviewer #2: "We consider it to be out of the scope of this paper to directly compare the two instruments against each other. Instead our goal is to demonstrate the suitability of the described instrument, given the calibration approach and post-processing described herein, for airborne observations with the ultimate goal of inferring local to regional fluxes. The instrument has advantages and drawbacks when directly compared to CRDS analyzers. One of the drawbacks is the reduced absorption path length. A big advantage is the large number of simultaneously sampled species using a single instrument. Depending on the scientific objective of the aircraft campaign, the additional measurements can either facilitate source attribution of observed methane enhancements (e.g. using ethane and/or nitrous oxide)), or

will allow to study specific scientific questions related to N2O, since there is no dead time in between each single measurement. This is especially useful for measurements in close vicinity to sources where plumes are only weakly dispersed (spatially narrow). While there is a certain chance of missing narrow plume structures with sequentially probing instruments, this QCL/ICL spectrometer does not suffer from such a problem. This is further described in Sect. 5. We included the motivation for the choice:
"[...] This particular analyzer has been favored over other instruments for its simultaneous multi-species capability and its sampling pattern, allowing the detection and quantitative observation of spatially narrow plumes. [...]"

4. **In the same context, it is also not obvious in the present form, why the authors decided for an extensive calibration scheme and additional data post-processing instead of developing a purged and sealed enclosure around the instrument. Apparently, most of the relevant drifts or biases are due to ambient air (H2O mainly) absorptions outside the multi-pass cell.**
We do agree that a pressure-stabilized and zero-air-flushed compartment would certainly be a significant improvement. However, this might be a simpler task for ground- or lab-based instruments but it is far more challenging for airborne instrumentation. With the current setup we are at the absolute mass limit to be able to acquire FAA certification. An additional pressurized compartment would at least mean some additional weight, not to mention the required flushing gas. It is also unsure if such a compartment would solve most of the problems. We fear that this might improve things but not completely solve all related problems because of the very sensitive apparatus involved and the harsh environment aircraft deployment poses. In this context we agree with Alan Fried, who commented on this in a previous review: "For example, some of the dependence is due to the changing mixing ratios for the species under study in the open-air path. Additional dependencies result from movement of optical windows and other components and are instrument dependent. Also, we find that the rate of cabin pressure change is an important factor, and this is specific to the particular aircraft and the flight pattern employed."

5. **Considering that the spectral retrieval software of the manufacturer has been around for more than 20 years, supporting a large number of custom-built instruments applied in a wide range of applications, one would assume that the software experienced a continuous development and incorporates many fine-tuning/customizing features in order to optimize also the fitting process. Therefore, it is highly interesting and valuable if the custom retrieval software (JFIT) significantly improves the performance. This must, however, be more clearly documented by a side-by-side comparison of the results of both software packages. Especially, the additional shift parameters introduced by JFIT and its co-allocation to various segments of the spectral window seems rather subjective and should be quantified in terms of performance improvements. The authors refer to Fig.8 (p13) to show that the tuning rate of the lasers is stable, which seems to be in contradiction with the many shift parameters introduced in JFIT.**
The spectral retrieval software provided by the manufacturer certainly is a very powerful tool and as you say, it implements lots of tuning and tweaking features that can be used for optimization of the retrieval process. We do not claim to provide a better software package, instead we purposely wrote our own retrieval software mainly to learn about possible modifications and to be able to easily adapt our code to new problems. The handling of the shift parameters is one such example. We are not sure of how that could have been done other than writing our own software. We think that it makes perfect sense to split the shift parameters on the spectral axes. Even though spectral shifts seem perfectly co-linear tiny shifts can have significant influence on the retrieved mixing ratios.

6. **Similarly, the discussion of the water vapor correction should contain further details about the observed biases and drifts in the whole range of water concentrations experienced during flights. Measuring water concentration at absolute level is challenging, so the authors should show the observed correlation between generated humidity and spectroscopically measured water mixing ratios. Also, some discussion is required to make clear how the additionally introduced broadening effect improves the measurements, and compare this to the impact of the significant spectral instability (10-3 cm-1) and potential temperature fluctuations of the sampled gas and of the cabin during flights.**
We are aware that measuring water concentrations at absolute levels certainly is a difficult task. We purposely do not

mention water vapor in the title because for us water vapor is just a side product used to enable reporting dry-air mixing ratios. The referred section mainly describes how the water vapor foreign broadening coefficient is obtained. This does not involve measuring water vapor at absolute levels, instead it is only necessary to span the range of atmospheric H_2O. The correlation for actual atmospheric measurements can be seen from the lowest panel in Fig. 10. We slightly modified the section to make this more clear and also to discuss how the broadening effect improves the measurements.
"[...] partial pressure of water vapor p_{H_2O} and the water broadening coefficient γ_{H_2O}. The former can be computed from the measured water vapor concentration. The latter can be empirically determined. Not including the self and water foreign broadening leads to relative errors in the range of 0-2% for the described setup, depending on the species of interest. While small for C_2H_6 and CH_4 with $< 0.03\%$, the influence on retrieved CO is rather large with $\sim 2\%$. In order to obtain γ_{H_2O} two MFCs are used to modify mixing ratios of water vapor in a clean and dry calibration gas. This does not involve measuring water vapor at absolute levels, instead it is only necessary to span the range of atmospheric H_2O. An additional downstream pump allows, in combination with a manually-controlled needle-valve, tuning the absolute pressure at the instrument inlet to simulate altitude changes. For these tests, the QCLS instrument has been operated at low flow rates of approx. $1 SLPM$ due to limitations on the two mass flow controllers. The water broadening coefficient γ_{H_2O} has been adjusted iteratively until reported dry-air mixing-ratios of the species of interest remained constant for the set of water vapor mixing ratios. [...]"

7. **Since the instrument is a unique platform, where two different mid-IR laser sources are operated side-by-side, a more detailed comparison of performances and noise characteristics of QCL/ICL would certainly be an added value to the manuscript.**
We sincerely agree, that this would be a very interesting analysis and a nice added value to the manuscript. However, this kind of study is out of the scope of this paper. This is something that should be carried out by laser experts and not as an addendum to this paper. We think this to deserve a publication on its own.

Specific comments:

1. **Pg2, L27: need more clarification what is meant by sequential and truly concurrent sensing. Otherwise, there should be a short note about the importance/benefit of measuring at 0.5 Hz instead of 2 Hz.**
In this context "concurrent sensing" is used to describe the fact, that the individual species are measured quasi-simultaneaously. The laser sweeps over the absorption lines with a frequency of 1.5kHz, resulting in a sampling of the spectral absorption of all targeted species at the same frequency. This is to be seen as opposed to "sequential" measurements, where one species is sampled after the other. Further details on the "sequential" approach are given in Section 5. To clarify this, we changed the relevant sentence to:
"[...] Unlike many established instruments measuring different species sequentially (one species after the other), the described spectrometer allows for concurrent sensing of the selected species and faster response times. Fast system response times are valuable to resolve the high variability in trace gases near strong sources. [...]"

2. **Pg2, L25: a reference to the paper at this stage is enough; especially, that Section 2 starts with the same information.**
The relevant sentence was redundant and has been removed in a revised version of the mansucript.

3. **Pg2, L29-31: How to interpret these cited works? In the present context, they give the impression that there is no open question regarding the suitability of QCLS for airborne measurements.**
We rephrased the corresponding text in the introduction to:
"[...] . Santoni et al. (2014) describe the successful deployment and evaluation of a similar airborne spectrometer (Harvard QCLS) for more than 500 flight hours. In contrast, Pitt et al. (2016) reported a severe cabin pressure dependency of their N_2O and CH_4 measurements using a commercial instrument (Aerodyne QCLS). By implementing a pressure-differentiated calibration method they were able to correct the corresponding data set, but had to omit roughly half of the measured data. Recently, Gvakharia et al. (2018) reported on a similar, clear cabin pressure dependency for their N_2O,

CO_2 and CO measurements (based on an Aerodyne QCLS). They suggested a fast calibration procedure to overcome these dependencies while maintaining a ≥ 90 % duty cycle. [...]"

4. **Pg2, L32: the main objective of the paper is missing. What is the final goal of this investigation? Which measurement data and for what purpose are they going to be used? Is the data quality adequate to answer the research questions?**
   We added the missing objective:
   "[...] The instrument is shown to provide airborne observations of high quality at high sampling rate with multi-species sensitivity as required for assessing greenhouse gas fluxes with a regional focus. [...]"

5. **Pg3, Sect 2.1: this section needs some re-work, e.g. statement like "optics compartment contains all optical elements" is redundant, while Laser#1 and #2 without clear definition has no sense. I suggest giving the driving specifications of the lasers (current and temperature) as well as their optical power output. Specify the exact detector type.**
   We have reworked this section to include the above mentioned:
   "[...] The spectrometer is split into an electronics compartment and an optics compartment. The electronics compartment includes an embedded computing system, thermoelectric cooling (TEC) controllers, power supplies, etc.. The optics compartment includes the lasers, the sample cell, the pressure controller, etc..

   Fig. 1 shows a top-view photograph of the optics compartment. A combination of a continuous wave (CW) QCL and ICL measures mixing ratios of CH_4, C_2H_6, CO_2, CO, N_2O and H_2O simultaneously by direct absorption spectroscopy. The sample cell is an astigmatic Herriott cell with approximate physical dimensions of 15cm x 15cm x 50cm (WxHxL) made from aluminum. It provides an effective absorption path length of $204\,\mathrm{m}$ with a net volume of $2.1\,\mathrm{L}$. Two laser light sources are tuned to a specific center wavelength by adjusting the temperature using Peltier elements contained in the lasers housing. Excess heat is removed through a liquid cooling/heating circuit (*SOLID STATE COOLING SYSTEMS, New York, USA*). Laser #1 is an Interband cascade laser manufactured by *nanoplus GmbH, Gerbrunn, Germany* with a peak output power of $9.5\,\mathrm{mW}$ operated at $4.7\,^{\circ}C$ and modulated between $2988.520\,cm^{-1}$ and $2990.625\,cm^{-1}$ using a linear current ramp of up to $40\,\mathrm{mA}$. Laser #2 is a quantum cascade laser manufactured by *ALPES Laser, St-Blaise, Switzerland* with a peak output power of $40\,\mathrm{mW}$ operated at $1.5\,^{\circ}\mathrm{C}$ modulated between $2227.550\,cm^{-1}$ and $2228.000\,cm^{-1}$ using a linear current ramp of up to $300\,\mathrm{mA}$. The lasers are modulated sequentially at a fixed frequency of $1.5\,kHz$. Laser #1 scans over absorption lines of CH_4, C_2H_6 and H_2O, Laser #2 sweeps over N_2O, CO_2 and CO lines. Each laser is sampled at 450 spectral points. Acquired spectra are co-added to yield a single output spectrum every half of a second. Before reaching the sample cell, the laser beam travels approximately $1.6m$ inside the instrument under ambient conditions. This will be referred to as the open-path of the instrument, which is heavily influenced by variations in cabin pressure, temperature and humidity during airborne operation. After passing through the sample cell, the combined output from both lasers hits a single TEC-cooled detector. A second, identical detector collects radiation from two auxiliary paths. The first auxiliary path contains a small, sealed reference cell filled with CH_4 and N_2O. This allows for spectral referencing during system startup. The second path introduces an etalon into the beam, allowing for experimental determination of the laser tuning rate, which relates laser supply current and emitted wavelength. [...]"

6. **Pg4, L1: obviously there are many hundreds of reflections within the multi-pass cell, which leads to significant decrease of optical power of the laser beam. What is the reflectivity of the mirrors and how much is the out-coupled ICL intensity?**
   The sample cell has not been modified from its original state. The exact reflectivity of the mirrors employed by Aerodyne Inc. is therefore unknown to us just like we did not measure the out-coupled intensity. From our point of view, this quantity is not relevant for the purpose of this manuscript. It is high enough to provide sufficient signal-to-noise ratio on the acquired spectra.

7. **Pg4, L3: I doubt that the laser devices are directly coupled to the Peltiers. There should be a buffer heat-sink between.**
   The laser devices are supplied by the manufacturer in a TO66 housing with the TECs already built in. This is what is

meant with "[...] Peltier elements directly attached to the laser [...]". We modified the relevant sentence accordingly:
"[...] Both lasers are tuned to a specific center wavelength by adjusting the temperature using Peltier elements contained in the laser housing. [...]"

8. **Pg8, L15: the relative frequency changes seem to be the same, which is also illustrated by Fig8. So what is the real benefit for using five different shift parameters?**
Even very subtle perturbations from the co-linearity of these shift parameters result in large changes in retrieved mixing ratios. Apart from that, the shift parameters provide a means for observing spectral stability, that would not be available otherwise.
"[...] This allows to properly model frequency changes and provides a means for observing spectral stability. Typical shift parameters for ground-based operation are given [...]"

9. **Pg9, L1: how large were the temperature fluctuations within the optical compartment? What was their effect on the spectral retrieval?**
The optical compartment is temperature stabilized by means of a recirculating chiller. As a consequence typical temperature fluctuations inside the optical compartment are on the order of $\sim 0.3\,\mathrm{K}$. We did not observe a correlation between retrieved mixing ratios and these fluctuations. We included this in the section on airborne performance:
"[...] We identified temperature fluctuations within ~ 0.3 K, pressure changes of up to ~ 200 hPa and relative humidity changes of up to 35 % in the instruments optical compartment during this flight. [...]"

10. **Pg9, Fig 9: specify the averaging time of the spectra.**
The averaging time of these spectra is $\tau = 0.5\,\mathrm{s}$. The values have been included in a revised version of the figure.

11. **Pg9, Fig 9: where is the CH4 line in the C2H6 fit-window? What is causing the strong bias in the residual in the CH4 fit-window?**
The bias in the residual of the CH4 window is the remainder of the third-order polynomial used to model the spectral baseline. The relevant sentence on Pg. 10 has been changed to:
"A single adjacent CH_4 line, located at $2989.981\,cm^{-1}$ has been included in order to obtain good C_2H_6 data even under these challenging conditions."

12. **Pg10, L7: a short clarification should be added why the authors chose this difficult spectral window? The range around 2224.5 cm-1 would, e.g. contain all the species with significantly less spectral interference. The ambition of getting the CO2 along with CO and N2O introduces severe compromises in the achievable spectral sensitivity and selectivity. Adding the fact that the selected CO2 line is not even the main isotopologue and seems to have large systematic bias, I seriously doubt whether this compromise is worthwhile.**
Thank you very much for hinting towards this spectral region. It seems to be a nice alternative. However, this region does neither include the primary CO2 isotopologue and CO2 absorption is smaller by approx. 30%. We do agree that CO seems to suffer less from spectral interference.

13. **Pg11, L9: indicate the precision and accuracy of the generated water vapor mixing ratios. What about hysteresis effects, i.e. humidifying vs. drying cycle?**
The relevant section might mistakenly give the impression that absolute water vapor concentrations are necessary to compute the water broadening coefficient. It is not. The water foreign broadening coefficient has been adjusted iteratively until reported dry-air mixing-ratios of the species of interest remained constant for the set of water vapor mixing ratios given the fixed concentrations in the calibration gas cylinder employed. We do not state how good our water vapor data actually is in terms of absolute values. Instead we just use the measured water vapor data to correct the species of interest. The cell has been flushed for a longer time with a given water vapor mixing ratio setpoint (on the order of minutes). From this we conclude, that the measurement cell was entirely flushed before every new setpoint. Hyteresis effects, i.e. humidifying vs. drying cycle should therefore have no influence.

14. **Pg12, L4: How well can the results obtained at 1 SLPM transferred to the 23 SLPM operation regim? What about simply using an empirical correction factor on the retrieved mixing ratios instead of introducing the broadening**

coefficient in the fitting procedure?
We think that the good agreement between the instruments presented in this work provides evidence enough, that the water broadening coefficients obtained at 1 SLPM can be transferred to the 23 SLPM regime. We further think that the water vapor correction approach used in this study reflects the relevant physical processes best. We did not try to use an empirical correction factor instead of the spectral approach, therefore we can't provide a statement on this.

15. **Pg12, Fig.7: it seems that the plot shows the deviation instead of variance. The Allan deviation plot indicates that the instrument drifts already after 30s even though operated under ground-based conditions. During flight, pressure and temperature variations, as well as mechanical vibrations tend to impair the performance of the instrument at even shorter time-scales. Considering the long-path of the optical cell, I wonder whether the authors did observe any correlated noise behavior when changing gas flow through the cell from 1 to 23 SLPM? As such, it would be useful to see the distribution diagram (or at least to give quantitative estimates of their spread) of the calibration gas measurements during flights.**
Thanks for pointing towards the wrong units in this figure. We did not observe a clearly correlated noise behavior when changing from low to high flow rates. The distribution diagram of the calibration gas measurements has been included in a supplement to the manuscript.

16. **Pg13, L9: what is meant by software based frequency lock mechanism?**
The way the frequency lock mechanism is implemented here is that the laser temperature is regulated to compensate for drifts using the spectral shift as the controller input and the current to the Peltiers as controller output. The controller itself is implemented in software on the data analysis computer.

We included this in the text:
"[...] Software based frequency lock refers to a controller regulating the laser temperature to compensate for drifts using the spectral shift as the controller input and the current to the Peltiers as controller output. The controller itself is implemented in software on the data analysis computer. [...]"

17. **Pg13, Fig8: what is the influence of the sudden frequency shift discontinuities on the retrieved mixing ratios?**
Using the spectral shift handling described within this work, the spectral shift discontinuities observed do not have a conspicuous effect.

18. **Pg17, L4: what would be the required isotopic composition of such a CO2?**
The required isotopic composition of such a CO2 would be 98.447% primary isotopologue and 1.079% secondary isotopologue ($^{13}C^{16}O_2$)
"[...] In this study we used working standards of synthetic nature from *Air Liquide*. Usually these are produced with CO_2 from natural gas & oil combustion processes. We determined the CH_4 and CO_2 values of each working standard gas cylinder using a NOAA-anchored (Cert.-Nr. CB11361) Picarro G-1301m. This has the drawback that we do not know the isotopic composition of our working standards as its impact had been considered negligible, e.g. (Chen et al., 2010). We only found out during development of JFIT, that the instrument is using a $^{13}C^{16}O_2$ line to derive ambient CO_2. We estimate the required isotopic composition of such a CO_2 to be 98.447% primary isotopologue and 1.079% secondary isotopologue or $\delta^{13}C = -19.6\,‰$ which seems reasonable according to B. Coplen et al. (2002). Since we are reporting retrieved mole fractions relative to the WMO scale, only the working standard reproducibility contributes to the total uncertainty of CH_4. Uncertainty on CO_2 is difficult to assess here because of the unknown isotopic composition in our working standards. [...]"

19. **Pg17, L8: give an estimate of the overall calibration gas consumption for the 18 flights and shortly discuss options for optimization.**
The overall calibration gas consumption for the 18 research flights amounts to $\sim 3.5\,m^3$. A reduction in necessary calibration gas aswell as a significant increase in system response times could be achieved by reducing the physical sample cell volume. We included the overall calibration gas consumption estimate in the revised manuscript:
"[...] calibration strategy from Sect. 2.3. This required a total calibration gas amount of $\sim 3.5\,m^3$ (excluding zero air) for the 18 research flights. [...]"

20. **Pg19, L10: as mentioned earlier, it would be useful in this context to show the distribution diagram of the calibration gas measurements performed at every 10 min interval and representing about 10% of the measurement time.**
The distribution diagram of the calibration gas measurements has been included in a supplement to the manuscript.

21. **Pg19, L17: it is somehow unclear what applies: in the previous section (pg18, L2) the authors claim that they were unable to reproduce the cabin pressure dependence, but in the conclusion is argued that the known cabin-pressure dependencies are effectively minimized by frequent two-point calibration.**
The relevant part of Pg18 was misleading, we therefore rephrased to:
"[...] A severe cabin pressure dependence in excess of $0.3 ppb hPa^{-1}$ in CH_4 mixing ratio has been previously reported for airborne TILDAS instrumentation (Pitt et al., 2016). This instrumentation however physically differs from the one reported here. It is not possible to accurately compare the dependencies of one instrument relative to another since many factors/quantities involved are instrument-specific, e.g. the open-path length, the positioning and properties of optical elements, like windows and mirrors, the stiffness and thermal expansion coefficients of employed optical stands, etc.. We were nevertheless able to effectively minimize cabin pressure dependencies during operation of the QCLS instrument aboard the C130 using the calibration strategy from Sect. 2.3. [...]"

22. **Pg19, L24: was the frequency lock mechanism active during flight operation only? Do the frequency-"jumps" correlate with laser heat-sink temperature changes?**
The frequency lock mechanism is always turned on following an initial referencing after instrument startup. We do not see a correlation with laser operating temperature. We did further not directly measure the laser heat-sink temperature nor did we log the recirculating chillers temperature either. This however is a very interesting question with respect to the source of the observed discontinuities that we will try to address soon.

23. **Pg20, L2: Having an uncertainty of 1 ppm and systematic bias of 10 ppm on the CO2 retrieval, projecting towards isotope ratio measurement is quite steep.**
If you want to express that it will be quite a challenge to reach isotope ratio measurements than we fully agree.

Technical corrections:

1. **Pg1, L12: "truly" is not a proper attribute for simultaneous. Remove it.**
"truly" has been removed.

2. **Pg2, L15: check reference, because Santoni et al. used QCLS instead of CRDS**
Here, we are referring to established IR spectrometers in general. The wording has been changed accordingly to:
"[...] used for airborne research, e.g. established IR spectrometers [...]"

3. **Pg2, L20: as above, Richter et al. used DFG instead of QCL**
The sentence has been changed to:
"[...] reported on a custom-built difference frequency generation (DFG) absorption spectrometer [...]"

4. **Pg3, L16: here and across the manuscript add space between value and unit. Also the chemical formula should be always printed in Roman (upright) type (see e.g. IUPAC Green Book).**
This has been implemented in a revised version of the manuscript.

5. **Pg4, L3: avoid using laser diode when referring to ICL/QCL devices.**
This comment has been taken into account in the revised version of the manuscript.

6. **Pg8, L4: replace "micro" by "fit" window.**
Occurences of "micro window" have been replaced with "fit window" in a revised version of the manuscript.

7. **Pg21, references: check for typos and completeness, e.g. at L10, L13, L22, etc.**
The reference pages have been checked for typos and completeness in a revised version of this manuscript.

~~Modification, Characterization~~ Adaptation and ~~Evaluation~~ performance assessment of a Quantum / Interband Cascade Laser Spectrometer for simultaneous airborne in situ observation of CH4, C2H6, CO2, CO and N2O

Julian Kostinek[1], Anke Roiger[1], Kenneth J. Davis[3], Colm Sweeney[6], Joshua P. DiGangi[5], Yonghoon Choi[5,7], Bianca Baier[6,8], Frank Hase[4], Jochen Groß[4], Maximilian Eckl[1], Theresa Klausner[1], and André Butz[2]

[1]Deutsches Zentrum für Luft- und Raumfahrt, Institut für Physik der Atmosphäre, Oberpfaffenhofen, Germany
[2]Institute of Environmental Physics, University of Heidelberg, Heidelberg, Germany
[3]Department of Meteorology and Atmospheric Science, The Pennsylvania State University, University Park, PA 16802, USA
[4]Institute of Meteorology and Climate Research, Karlsruhe Institute of Technology, Karlsruhe, Germany
[5]NASA Langley Research Center, Hampton, VA 23681-2199, USA
[6]NOAA ESRL Global Monitoring Division, Boulder, CO 80305-3328, USA
[7]Science Systems and Applications, Inc., Hampton, VA 23681, USA
[8]Cooperative Institute for Research in Environmental Sciences, University of Colorado Boulder, Boulder, CO 80305, USA

Correspondence: Julian Kostinek (julian.kostinek@dlr.de)

Abstract. ~~Achieving an improved understanding of the anthropogenic influence on climate due to man made greenhouse gas emissions is of major interest for the global civilization. Sources, sinks and transport of climatologically-relevant gases in the Earth's atmosphere are still insufficiently understood, implying a fundamental need for accurate, spatially and temporally dense observations. Tunable diode laser~~ Tunable laser direct absorption spectroscopy is a widely used technique for in situ sensing of atmospheric composition. ~~Mid-infrared spectrometers have become commercially available, since continuous wave quantum cascade (QCL) and interband cascade lasers (ICL) today achieve excellent performance, stability and high output power at typical ambient conditions.~~ Aircraft deployment poses a challenging ~~environment for these newly-developed instruments~~ operating environment for instruments measuring climatologically-relevant gases in the Earth's atmosphere. Here, we demonstrate the successful adaption of a commercially available ~~QCL/ICL~~continuous wave quantum cascade (QCL) and interband cascade laser (ICL) based spectrometer for airborne in-situ trace gas measurements with a local to regional focus. The instrument measures methane, ethane, carbon dioxide, carbon monoxide, nitrous oxide and water vapor simultaneously, with high 1s-1σ ~~precision (740 ppt, 205 ppt, 460 ppb, 2.2 ppb, 137 ppt, 16 ppm~~precision (740 ppt, 205 ppt, 460 ppb, 2.2 ppb, 137 ppt, 16 ppm, respectively) and high frequency (~~2 Hz~~2 Hz). We estimate a total ~~measurement uncertainty of 2.3 ppb, 1.6 ppb, 1.0 ppm, 7.4 ppb and 0.8 ppb in CH_4, C_2H_6, CO_2, CO and N_2O~~1s-1σ uncertainty of 1.85 ppb, 1.6 ppb, 1.0 ppm, 7.0 ppb and 0.8 ppb in CH_4, C_2H_6, CO_2, CO and N_2O, respectively. The instrument enables ~~truly~~ simultaneous and continuous ~~(zero dead-time)~~ observations for all targeted species. Frequent calibration allows for a measurement duty cycle $\geq 90\%$~~while retaining high accuracy.~~ . A custom retrieval software has been implemented and instrument performance is reported for a first field de-

ployment during NASA's Atmospheric Carbon and Transport America (ACT-America) campaign in fall 2017 over the eastern and central U.S.. This includes an inter-instrumental comparison with a calibrated cavity ring-down greenhouse gas analyzer (operated by NASA Langley Research Center, Hampton, USA) and periodic flask samples analyzed at the National Oceanic and Atmospheric Administration (NOAA). We demonstrate ~~excellent~~ good agreement of the QCL/ICL based instrument to these concurrent observations within the combined measurement uncertainty ~~.~~ after correcting for a constant bias. We find that precise knowledge of the $\delta^{13}C$ of the working standards and the sampled air is needed to enhance CO_2 compatibility when operating on the 2227.604 cm^{-1} $^{13}C^{16}O_2$ absorption line.

1 Introduction

With steadily increasing greenhouse gas concentrations in the Earths atmosphere an improved understanding of the anthropogenic influence on climate is of major interest for the global civilization. Globally averaged carbon dioxide (~~CO_2) mixing ratios~~ CO_2) mole fractions have increased by 40% since 1750. Methane (~~CH_4) mixing ratios~~ CH_4) mole fractions have more than doubled since the pre-industrial era, where over 60% of this increase is estimated to be of anthropogenic nature ~~(IPCC, 2014)~~(Ciais et al., 2013). Nitrous oxide (~~N_2O~~N_2O) is a strong greenhouse gas and is expected to ~~remain~~ have the most important ozone-depleting anthropogenic impact throughout the 21st century (Ravishankara et al., 2009). Ethane (~~C_2H_6~~C_2H_6) is a powerful tracer commonly used to discriminate between different types of methane sources (Smith et al. (2015); Barkley et al. (2017); Peischl et al. (2015)) and carbon monoxide (~~CO~~CO) is a marker for incomplete combustion processes and relates to the formation of tropospheric ozone (Klemm et al., 1996).

Aircraft provide a flexible ~~basis~~ platform for satisfying the fundamental need for accurate, temporally and spatially dense observations of these climatologically-relevant gases from local to regional scales. On-board meteorological data acquisition systems allow for concurrent observations of important atmospheric state variables like the local wind field, which is particularly useful to estimate ~~emission fluxes~~emissions. Spectroscopic instruments making use of molecular ro-vibrational absorption allow for high temporal coverage through fast instrument response times (Chen et al., 2010). Some have already been used for airborne research, e.g. ~~well-established cavity ring-down instruments~~ established IR spectrometers (O'Shea et al. (2013); Santoni et al. (2014); O. L. Cambaliza et al. (2015); Filges et al. (2015)). Significant effort led to instruments operating in the mid infrared (IR) region, e.g. liquid nitrogen cooled lead-salt diode laser based spectrometers (Fried and Richter, 2007). With the commercial availability of continuous-wave lasers emitting in the mid ~~infrared (IR)~~ IR region near ambient temperature (Capasso (2010); Vurgaftman et al. (2015); Kim et al. (2015), Beck et al. (2002)) several new instrument designs have emerged (McManus et al. (2015); Zellweger et al. (2016)). QCL/ICL based systems exploit several orders of magnitude stronger molecular absorption features in the mid infrared compared to near infrared based ~~cavity ring-down~~ instruments. Richter et al. (2015) reported on a custom-built ~~QCL~~ difference frequency generation (DFG) absorption spectrometer for simultaneous in-situ detection of formaldehyde (~~CH_2O) and C_2H_6 providing best-in-class~~ CH_2O) and C_2H_6 providing high detection sensitivities of ~~40 *ppt* and 15 *ppt*~~40 ppt and 15 ppt, respectively. The custom-built airborne QCL spectrometer described by Catoire et al. (2017) allows for simultaneous observation of ~~CO, CH_4~~ CO, CH_4 and nitrogen dioxide (~~NO_2~~NO_2) with in-flight precisions of ~~0.3 *ppb*, 5 *ppb* and 0.3 *ppb*~~ 0.3 ppb, 5 ppb and 0.3 ppb for a sampling time of ~~1.6 *s*~~1.6 s. McManus et al. (2011) reported on the development of a high-sensitivity trace gas instrument based on quantum cascade lasers and astigmatic Herriott cells with up to ~~240 *m*~~ 240 m path length. ~~This design is commercially available from *AERODYNE RESEARCH INC., Billerica, USA*, and allows for simultaneous observation of a multitude of gases, depending on the wavelength of the installed lasers.~~ Unlike many established ~~cavity ring-down~~ instruments measuring different species sequentially (one species after the other), the described spectrometer allows for ~~truly~~ concurrent sensing of the selected ~~observables~~ species and faster response times. These instruments have already been operated on different research aircraft. ~~Santoni et al. (2014) reported on overall instrument performance for over~~ Santoni et al. (2014) describe the successful deployment and evaluation of a similar airborne

spectrometer (Harvard QCLS) for more than 500 flight hours. ~~Pitt et al. (2016) found a strong cabin pressure dependence on retrieved methane mixing ratios.~~ However, Pitt et al. (2016) reported a severe cabin pressure dependency of their N_2O and CH_4 measurements using a commercial instrument (Aerodyne QCLS). By implementing a pressure-differentiated calibration method they were able to correct the corresponding data set, but had to omit roughly half of the measured data. Recently, Gvakharia et al. (2018) ~~described a fast calibration strategy to overcome this cabin pressure dependence.~~ reported on a similar cabin pressure dependency for their N_2O, CO_2 and CO measurements (based on an Aerodyne QCLS). They suggested a fast calibration procedure to overcome these dependencies while maintaining a $\geq 90\%$ duty cycle.

Here, we describe the setup and performance of our flight-proven (over 100 flight hours) airborne QCL/ICL system developed for simultaneous airborne measurements of ~~CH_4, C_2H_6, CO_2, CO, N_2O and H_2O.~~ CH_4, C_2H_6, CO_2, CO, N_2O and H_2O. The instrument is shown to provide multi-species airborne observations for assessing greenhouse gas fluxes with a local (e.g. single facilities) to regional focus (e.g. urban agglomerations). Simultaneous observations of CH_4 and C_2H_6 facilitate to pinpoint sources of CH_4 enhancements (Smith et al., 2015). At the same time, the instrument provides measurements of N_2O, the third most important greenhouse gas. This makes the instrument an ideal tool for airborne quantification and source attribution of greenhouse gas emissions using e.g. the aircraft based mass balance approach. Section 2 summarizes the refinements over the commercial system for use on aircraft. We show that frequent two-point calibration can mitigate cabin pressure dependencies. Section 3 describes our custom-built retrieval software developed for tuning the retrieval process~~to yield optimum output~~. Sections 4 and 5 report on instrument performance in the laboratory and in the field during NASA's ACT-America fall 2017 campaign, ~~respectively,~~ including an inter-instrumental comparison with a calibrated cavity ring-down instrument and periodically taken flask samples. Section 6 summarizes our findings and concludes the study.

2 The airborne DLR QCL/ICL spectrometer

The spectrometer system used here builds upon the *Dual Laser Trace Gas Monitor*, a commercial tunable IR laser ~~diode~~ direct absorption spectrometer (TILDAS) available from *AERODYNE RESEARCH INC., Billerica, USA*~~.~~, acquired by *Deutsches Zentrum für Luft- und Raumfahrt* (DLR) in late 2016. The basic instrument has already been extensively described in McManus et al. (2011). We will therefore only briefly introduce the basic instrument setup followed by a description of the refinements required to operate the instrument on research aircraft.

2.1 Basic instrument setup

The spectrometer is split into an electronics compartment and an optics compartment. The electronics compartment includes an embedded computing system, thermoelectric cooling (TEC) controllers, power supplies, etc.. The optics compartment includes the lasers, the sample cell, the pressure controller~~and all optical elements.~~

~~Top-down photograph on the optics compartment (left panel). The sample cell made from aluminum along with the pressure controller and pressure transducers can be identified in the lower half. The QCL/ICL lasers are mounted inside the blue housings to the left of the collimating Schwarzschild telescopes in the two black housings. The two detectors are mounted below the~~

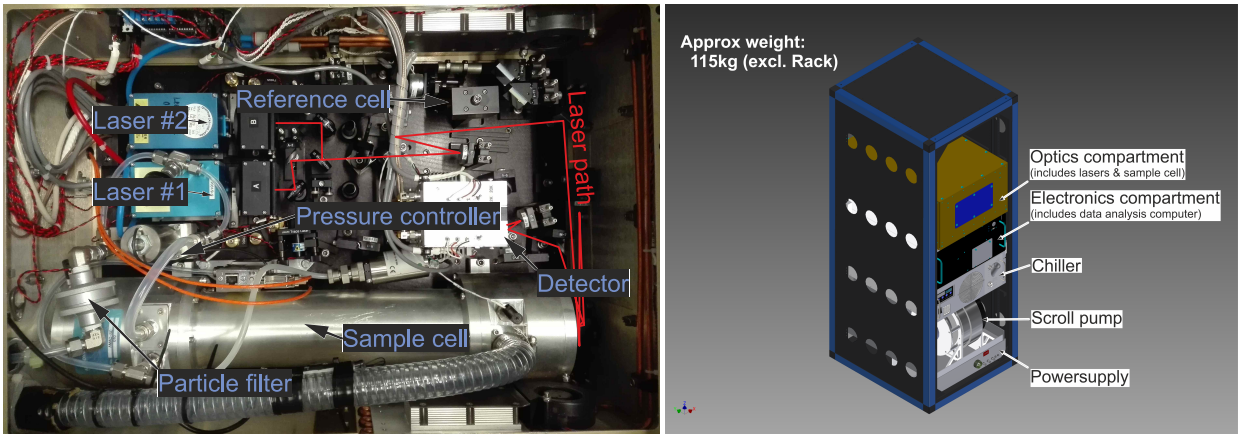

Figure 1. Top-down photograph on the optics compartment (left panel). The sample cell made from aluminum along with the pressure controller and pressure transducers can be identified in the lower half. The QCL/ICL lasers are mounted inside the blue housings to the left of the collimating Schwarzschild telescopes in the two black housings. The two detectors are mounted below the silver aluminum cases, housing the pre-amplifiers, on the right. The first detector is used for detecting both lasers after passing through the sample cell. The second detector is used for spectral referencing through an auxiliary optical path. The right panel illustrates the rack mounted instrument. The figure includes solid models from Aerodyne Inc. and Solid State Cooling Systems.

~~silver aluminum cases, housing the pre-amplifiers, on the right. The first detector is used for detecting both lasers after passing through the sample cell. The second detector is used for spectral referencing through an auxiliary optical path. The right panel illustrates the rack mounted instrument.~~ ~~Fig.~~ , etc.. Figure 1 shows a top-view photograph of the optics compartment. A combination of a continuous wave (CW) QCL and ICL measures ~~mixing ratios of CH_4, C_2H_6, CO_2, CO, N_2O and H_2O~~ mole fractions of CH_4, C_2H_6, CO_2, CO, N_2O and H_2O simultaneously by direct absorption spectroscopy. The sample cell is an astigmatic Herriott cell with approximate physical dimensions of ~~15cm x 15cm x 50cm~~ 15 cm x 15 cm x 50 cm (WxHxL) made from aluminum. It provides an effective absorption path length of ~~204m~~ 204 m with a net volume of ~~2.1L~~2.1 L. Two laser light sources ~~emit in the mid-IR region, specifically around 3.3μm for Laser #1 and 4.5μm for Laser #2. Both lasers~~ are tuned to a specific center wavelength by adjusting the operating temperature using Peltier elements ~~directly attached to the laser diodes~~contained in the lasers housing. Excess heat is removed through a liquid cooling/heating circuit (*SOLID STATE COOLING SYSTEMS, New York, USA*). ~~Operating temperatures are 4.7°C for~~ Laser #1 is an Interband cascade laser manufactured by *nanoplus GmbH, Gerbrunn, Germany* with a peak output power of 9.5 mW operated at 4.7 °C and modulated between 2988.520 cm^{-1} and ~~1.5°C for Laser #2, respectively. A~~ 2990.625 cm^{-1} using a linear current ramp ~~drives sequential spectral modulation at a fixed frequency of 1.5kHz~~of up to 40 mA. Laser #~~1 is tuned between 2988.520cm^{-1} and 2990.625cm^{-1}. The second laser is tuned between 2227.550cm^{-1} and 2228.000cm^{-1}~~2 is a quantum cascade laser manufactured by *ALPES Laser, St-Blaise, Switzerland* with a peak output power of 40 mW operated at 1.5 °C modulated between 2227.550 cm^{-1} and 2228.000 cm^{-1} using a linear current ramp of up to 300 mA. The lasers are modulated sequentially at a fixed frequency of 1.5 kHz. Laser #1 scans over absorption lines of ~~CH_4, C_2H_6 and H_2O, the second laser sweeps over N_2O, CO_2 and CO~~ CH_4,

C_2H_6 and H_2O, Laser #2 sweeps over N_2O, CO_2 and CO lines. Each laser is sampled at 450 spectral points. Acquired spectra are co-added to yield a single output spectrum every half of a second. Before reaching the sample cell, the laser beam travels approximately ~~1.6m~~ 1.6 m inside the instrument under ambient conditions. This will be referred to as the open-path of the instrument, which is heavily influenced by variations in cabin pressure, temperature and humidity during airborne operation. After passing through the sample cell, the combined output from both lasers hits a single TEC-cooled detector. A second, identical detector collects radiation from two auxiliary paths. The first auxiliary path contains a small, sealed reference cell filled with ~~CH_4 and N_2O~~CH_4 and N_2O. This allows for spectral referencing during system startup. The second path introduces an etalon into the beam, allowing for experimental determination of the laser tuning rate, which relates laser supply current and emitted wavelength.

2.2 Refinements for airborne operation

The key challenges for a successful deployment on research aircraft are limited space and power, the occurrence of linear and angular accelerations and large pressure, temperature and humidity fluctuations in both cabin and sampled air. Airborne instrumentation further requires a fast system response time, owing to the rapid movement of aircraft in the atmosphere. The response time is controlled by the time it takes to completely exchange the air in the sample cell which is driven by the highest achievable volumetric flow rate given a specific pump and sample cell volume.

Here, a scroll pump has been chosen to enable a constant sample flow through the sample cell. The lubricant-free scroll pump runs very smoothly, avoiding injecting large vibrations into the measurement system, yet providing good pumping performance with a nominal value of 500 liters per minute at standard conditions. This translates to a net flow rate of ~~25 *SLPM*~~ 25 SLPM when operating with a cell pressure of ~~50 *hPa*~~50 hPa. Earlier experience showed that large electrical inrush currents have jeopardized nominal system startup (priv. comm. Stefan Müller, MPI Mainz). Sudden power failure, due to over-current triggering aircraft circuit breakers, may lead to failures in the data analysis equipment. The original motor has therefore been exchanged with a synchronous three-phase motor (*BAUMUELLER NUERNBERG GMBH, Velbert, Germany*). This DC motor provides a rated power of ~~627 *W* at 28 *V DC*~~627 W at 28 VDC. By using a digital motor controller the maximum startup current can be limited amongst various other tuning options. From previous studies the motor is known to emit a considerable amount of heat; a forced airflow provided by a standard axial fan ensures motor temperatures stay in the rated range.

Aircraft deployment requires the entire system to operate with a maximum of ~~50 *A* at 28 *V DC*~~50 A at 28 VDC. Power consumption of the instrument is mainly dominated by the pump and the thermoelectric cooling making up more than 3/4 of the total power requirement. Both components have been electrically converted without the need for power inverters from ~~230 *V AC* to 28 *V DC*~~ 230 VAC to 28 VDC to increase overall efficiency. The spectrometer and its internal computer are driven by a power inverter.

Large parts of the wiring harness have been exchanged from standard PVC cables to aviation-grade fire-resistant wiring. Mandatory electromagnetic compatibility/interference (EMC/EMI) tests have been carried out to comply with Federal Aviation Administration (FAA) regulations. The rack-mounted instrument sums up to a total mass of ~~approx. 115 *kg*~~ approximately 115 kg and has been tested to withstand linear accelerations of up to ~~9 *g*~~ 9 g on the aircraft forward axis, ~~8 *g*~~ 8 g on the downward

axis, ~~6g~~ 6 g on the upward and ~~2.25g~~ 2.25 g sidewards. Due to aircraft certification issues, pure water is used as process fluid for the liquid cooling/heating circuit instead of the intended propylene glycol / water mixture.

A 3/8" inner diameter hose made out of Polytetrafluoroethylene (PTFE) has been chosen for the sample air intake as a compromise between pressure drop across the inlet and to minimize lag time between the inlet and the sample cell. Inside the instrument and upstream of the sample cell, an aerosol filter holds back particles bigger than ~~2 μm~~ 2 μm. The inlet is rear facing, preventing large particle entrainment and protecting the instrument from liquid water and ice. Owing to the small diameter, the intake flow is inside the turbulent regime at all times ($Re \sim 4000$).

Finally, the sample cell pressure is regulated by means of a fully-configurable pressure controller (*BRONKHORST High-Tech B.V., Ruurlo, Netherlands*). A chip-scale temperature-compensated pressure transducer (*Measurement Specialties (Europe), Ltd.*) and a humidity sensor (*Sensirion AG, Staefa ZH, Switzerland*) have been built into the optics compartment, to allow for monitoring the open path state variables (see section 2.1).

2.3 In-flight calibration strategy

A custom-built calibration system has been implemented as illustrated in ~~Fig.~~ Figure 2. Using mass flow controllers (MFCs, *BRONKHORST High-Tech B.V., Ruurlo, Netherlands*), two gases can be mixed at arbitrary ratios. The calibration gas mixture has been chosen to resemble "target" gas ~~mixing ratios~~ mole fractions close to atmospheric ambient ~~conditions~~values. The cylinders have been cross-calibrated using a Picarro CRDS against NOAA standards and are thus traceable to World Meteorological Organization (WMO) standards for ~~the species CH_4 and CO_2.C_2H_6, CO and N_2O~~ CH_4 (Cert.-Nr. CB11361, WMO X2004A for CH_4 (Dlugokencky et al., 2005)). C_2H_6, CO and N_2O are compared to NOAA flask samples taken during the ACT-America field campaigns, which are also traceable to WMO standards. We use ultra-pure synthetic air as "zero" gas instead of pure nitrogen (~~N_2~~N_2) to be in accordance with aircraft safety regulations and because the ~~mixing ratio~~ mole fraction of synthetic air (79.5% ~~N_2~~ N_2 and 20.5% ~~O_2~~O_2) is chemically closer to sampled atmospheric air. Our calibration setup allows the net flow rate from the calibration cylinders to be slightly higher than the sample flow rate, minimizing pressure variations in the sample cell during switchover from normal to calibration sampling. To avoid contamination with cabin air, leak tests have been carried out on a regular basis during the ACT-America field campaign. Typical calibration distribution diagrams are available in the Supplement Section 4.

Owing to the high sensitivity of the retrieved ~~mixing ratios~~ mole fractions to changes in ambient conditions during flights (Gvakharia et al., 2018), calibration cycles are carried out automatically every 5 to 10 minutes. Each cycle consists of a pre-programmed sequence of flushing the sample cell with zero gas for 10 seconds followed by another 10 seconds of calibration gas. These time intervals have been found to be a good compromise between calibration gas cylinder endurance and measurement duty cycle. ~~Furthermore, only a single MFC is active at the time~~ The online mixing feature is not used for in-flight calibration~~, reducing the uncertainty on the calibration gas mixing ratios to the uncertainties on the gas cylinders themselves~~. Hence, no dilution of the calibration standard with zero air is introduced during flights and the uncertainty in the flow rate measurements can be omitted. Online mixing (~~only~~ relevant for linearity checks~~, not for in-flight calibration~~) adds the uncertainty of the controlled mass flow ~~on top. Measured mixing ratios~~ (0.5 % relative error) on top of the gas cylinder

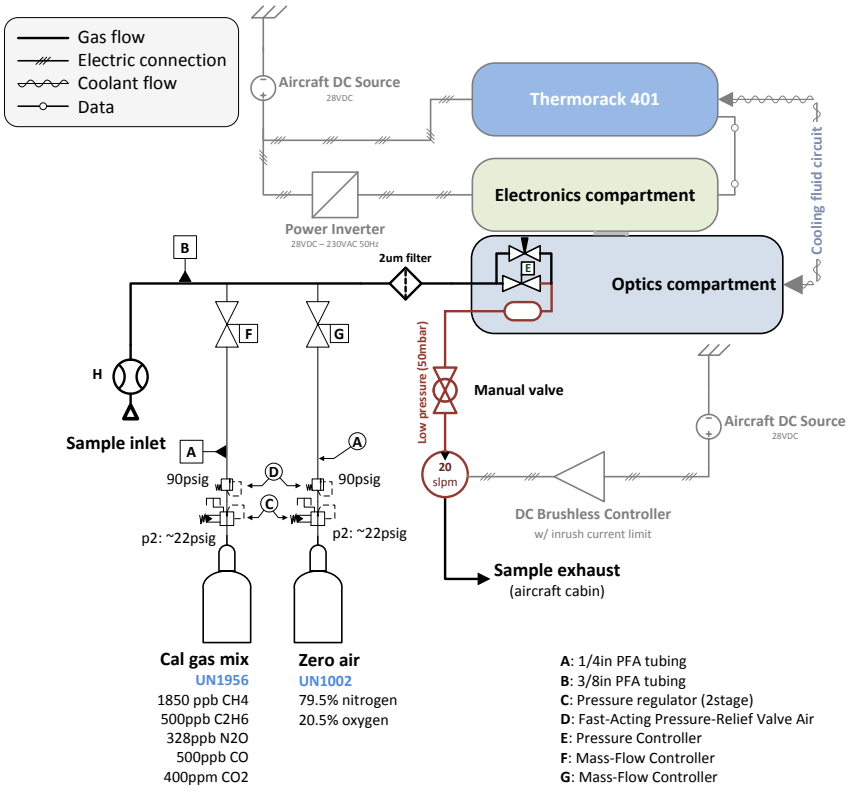

Figure 2. Schematic showing the main components with emphasis on the calibration system. A mass flow meter allows for measuring the sample flow rate. Two reference gases can be mixed at any arbitrary ratio by means of two calibrated mass flow controllers. A $2\mu m$ particle filter upstream of the sample cell avoids cell contamination.

uncertainties. Measured mole fractions of all detected species settle to an approximately constant value within the first two seconds after switchover from calibration gas to sample air and vice versa. The only exception is water vapor, which is observed to settle after ~~approx.~~ approximately 30 seconds because of its stickiness and because the inlet tubing is made out of PTFE. The observed decay in ~~H_2O~~ H_2O is different from the decay in other species in that a slow, almost linear decay follows the initial exponential decay, due to remaining water vapor in the inlet tubing and the sample cell.

3 Data Retrieval & Post-processing

The standard approach to retrieve dry-air ~~mixing ratios~~ mole fractions from the Aerodyne QCLS instruments is by making use of the software supplied by the manufacturer (TDLWintel). Here we utilize a custom retrieval software (JFIT) developed to double check the output of the TDLWintel software and to enhance the ability of tweaking the retrieval process~~to yield optimum~~

~~output.~~ . Our main goal in developing a stand-alone algorithm here, was to learn about possible error sources, mitigation possibilities of instrument dependencies and to be able to extend the instruments capabilities in the future.

The code is written in plain C++. It digests the sample cell pressure and temperature measurements to generate a synthetic spectrum based on line-by-line parameters from the HITRAN2012/HITRAN2016 (Rothman et al. (2013); Gordon et al. (2017)) database using a conventional Voigt profile approach. Ethane line-by-line data have been taken from high-resolution FTIR spectra due to deficiencies in the HITRAN data for this particular species/wavenumber combination (Harrison et al., 2010). The computation of the Voigt profile has been adopted from Abrarov and Quine (2015)~~for improved efficiency~~. Our retrieval code differs from the TDLWintel approach in the determination of the spectral baseline, the handling of shift parameters and open path water absorption. ~~TDLWintels spectral baseline is defined by manually positioned markers and shift parameters are specific for each species and coupled to a fingerprint absorption line (see Fig. 4). Determination of open path water absorption is only possible at one fixed pressure value.~~

A typical raw spectral output, as saved by the instrument in binary format is illustrated in ~~Fig. 3. A typical raw spectrum as recorded in binary format by the instrument. Arrows have been added to ease identification of the observed chemical species. Channel numbers on the abscissa can be converted to spectral units using the laser tuning rate. The intensity offset can be corrected by shifting the entire spectrum to yield zero intensity when lasers are turned off.~~ Figure 3. The two consecutive laser

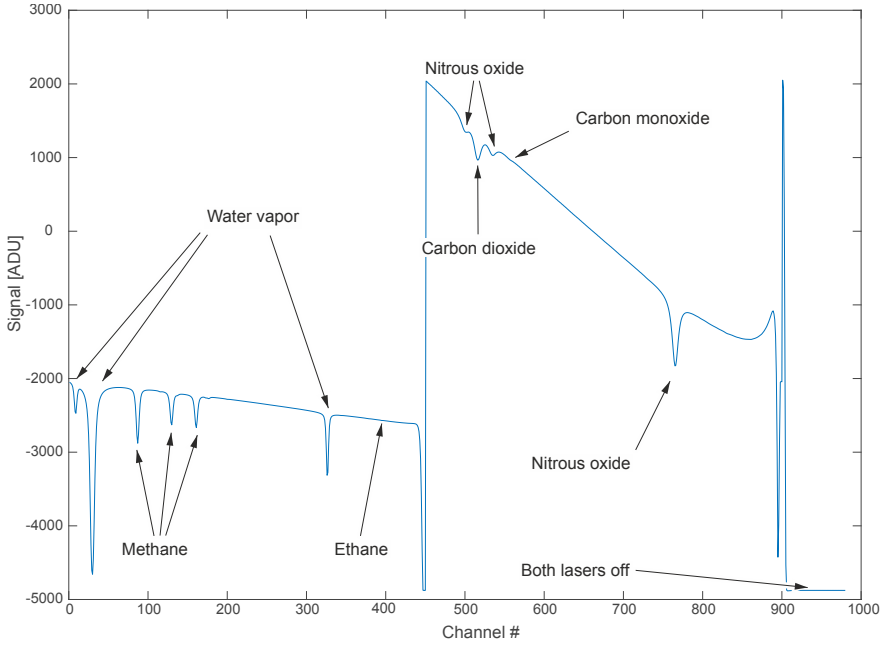

Figure 3. A typical raw spectrum as recorded in binary format by the instrument. Arrows have been added to ease identification of the observed chemical species. Channel numbers on the abscissa can be converted to spectral units using the laser tuning rate. The intensity offset can be corrected by shifting the entire spectrum to yield zero intensity when lasers are turned off.

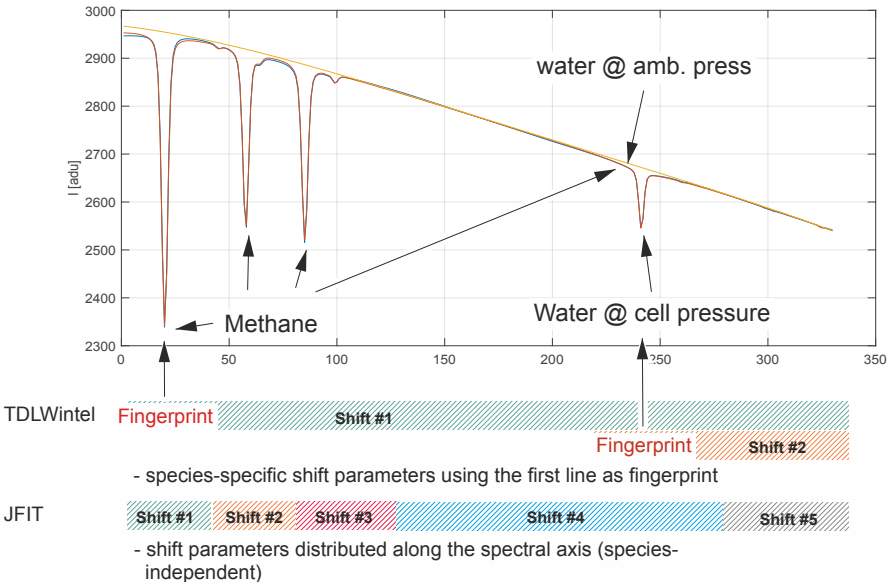

Figure 4. Schematic depicting the handling of spectral shift parameters and baseline modeling. The spectral baseline is fitted as a polynomial together with absorption features over the entire fit window. Shift parameters have been implemented in a species-independent way. Open-path water is also included in the model.

scans are clearly visible. On the left side, Laser #1 sweeps between ~~2988.520 cm^{-1} and 2990.625 cm^{-1}~~ 2988.520 cm^{-1} and 2990.625 cm^{-1} and hence, over absorption features of ~~CH_4, C_2H_6 and H_2O~~ CH_4, C_2H_6 and H_2O. The right side corresponds to the wavelength range of Laser #2 (~~2227.550 cm^{-1} to 2228.000 cm^{-1}~~ 2227.550 cm^{-1} to 2228.000 cm^{-1}) and includes absorption features of ~~N_2O, CO and CO_2~~ N_2O, CO and CO_2. After the lasers have scanned their full range, both lasers are completely turned off to allow for the determination of the detector zero-intensity offset. The abscissa corresponds to the individual sampling points, which can be converted to spectral units using the known laser tuning rate. The flat sections of the spectrum with no molecular absorption, are considered to represent the spectral baseline. The shape of this baseline is mainly controlled by laser characteristics, the detector response function and optical properties of the installed mirrors and windows inside the instrument.

The spectrum is broken down into 3 ~~micro~~ fit windows for the retrieval process (see ~~Fig.~~ Figure 5). These were chosen based on the best overall performance found in retrieval tests and named after the chemical species included. A synthetic spectrum, including a polynomial representing the spectral baseline, is generated and fitted using an unbounded Levenberg-Marquardt least-squares algorithm (Marquardt, 1963). The degree of the background-fitting polynomial has been adjusted empirically for each ~~micro~~ different fit window. Species independent shift parameters have been included allowing individual absorption features to freely move on the spectral axis. Special care has been taken to group weak and strong absorption features together in a single shift parameter, to provide sufficient certainty on their spectral positions. ~~Schematic depicting the handling of spectral~~

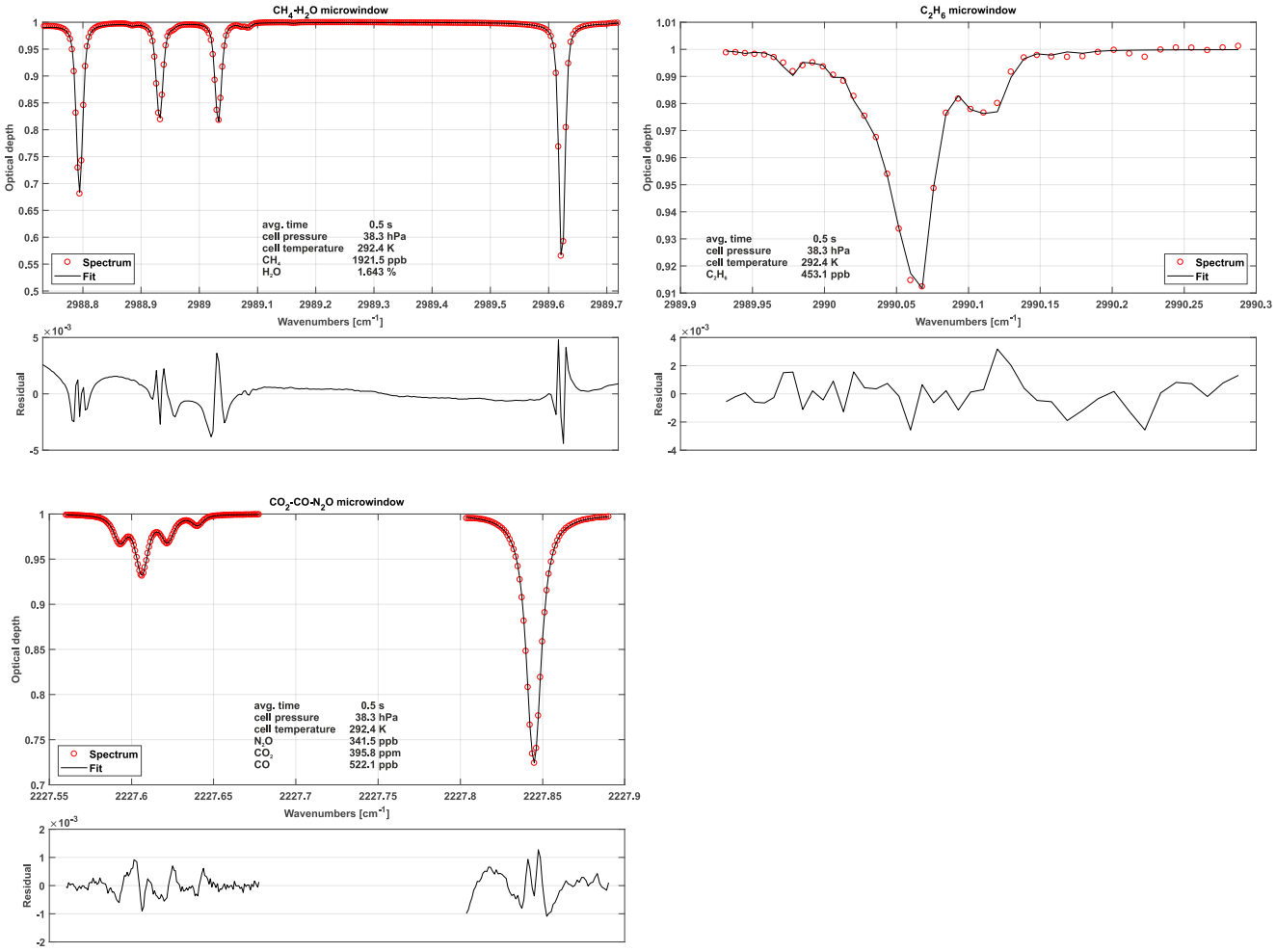

Figure 5. Typical, normalized spectra for each fit window including fits and associated residuals. The first fit window (top left) includes CH_4 and H_2O absorption features. The top right fit window depicts C_2H_6 absorption. The lower left spectrum shows CO, CO_2 and N_2O absorption.

~~shift parameters and baseline modeling. The spectral baseline is fitted as a polynomial together with absorption features over the entire micro window. Shift parameters have been implemented in a species-independent way. Open-path water is also included in the model.~~ In other words, not every absorption line has its own shift parameter, but they are grouped as schematically shown in ~~Fig.~~ Figure 4. As a result, only 5 shift parameters are included although the synthetic spectrum in ~~Fig.~~ Figure 4 is composed of more than 20 individual lines. When the absorptivity does not yield enough certainty to ensure proper determination of the shift parameters for a single spectrum, the shift variables are held constant at the mean over its last 10 values. If another species in the relevant ~~micro~~ fit window allows for a proper determination of the spectral position, remaining shift parameters

are coupled to those with enough certainty. This ~~strategy~~ allows to properly model ~~frequency changes between consecutive measurements~~absorption line center frequency changes and provides a means for observing spectral stability. Typical shift parameters for ground-based operation are given in ~~Fig.~~ Figure 8 for the ~~CH_4-H_2O and CO_2-CO-N_2O micro~~ CH_4-H_2O and CO_2-CO-N_2O fit windows. Pressure, humidity and temperature data obtained from within the optics compartment are used to model ~~H_2O~~ H_2O absorption at cabin pressure in the open-path region.

~~Typical, normalized spectra for each micro window including fits and associated residuals. The first micro window (top left) includes CH_4 and H_2O absorption features. The top right micro window depicts C_2H_6 absorption. The lower left spectrum shows CO, CO_2 and N_2O absorption.~~ The ~~CH_4-H_2O micro~~ CH_4-H_2O fit window covers almost the entire set of spectral features covered with Laser #1 except for the ~~C_2H_6~~ C_2H_6 absorption features. The spectral baseline is modeled as a third-order polynomial over the full range of the ~~micro~~ fit window. A typical spectrum including fit is depicted in ~~Fig.~~ Figure 5 along with typical spectra for the other two ~~micro~~ fit windows.

The ~~C_2H_6 micro~~ C_2H_6 fit window includes absorption features of ~~CH_4 and C_2H_6~~CH_4 and C_2H_6. The main challenge of retrieving precise ~~C_2H_6 mixing ratios~~ C_2H_6 mole fractions arises from its very low background concentration in the atmosphere (~~approx. 1.05 ppb~~ approximately 1.05 ppb in the northern hemisphere (Simpson et al., 2012)). A single adjacent ~~CH_4 line~~CH_4 line, located at 2989.981 cm^{-1} has been included in order to obtain ~~good C_2H_6~~ C_2H_6 data even under these challenging conditions. In this case, the weak ~~CH_4~~ CH_4 absorption is not modeled as a free parameter and is hence not used for retrieving the ~~CH_4 mixing ratio~~CH_4 mole fraction, but for localizing the spectral position / shift parameter of the ~~C_2H_6~~ C_2H_6 absorption feature in the absence of a clear ~~C_2H_6~~ C_2H_6 signal. The ~~CH_4 mixing ratios~~ CH_4 mole fractions are fixed to the values determined from the previous ~~micro~~ fit window. Using this approach, we found a clear improvement in the ~~C_2H_6~~ C_2H_6 data quality including a higher precision and the absence of discontinuities. The associated spectral baseline is modeled as a second-order polynomial.

The ~~CO_2-CO-N_2O micro~~ CO_2-CO-N_2O fit window covers the entire second laser and is the most complex spectral scene. It includes several overlapping absorption features making the retrieval of ~~mixing ratios~~ mole fractions of the targeted species challenging. As illustrated in ~~Fig.~~ Figure 5, a single ~~CO_2~~ CO_2 absorption line is surrounded by two ~~N_2O~~ N_2O lines. The ~~CO~~ CO line is directly adjacent to one of the ~~N_2O~~ N_2O lines. This results in comparatively large signal noise and ~~deteriorated accuracy on the retrieved mixing ratios~~ increased uncertainty in the retrieved mole fractions due to crosstalk between the ~~N_2O, CO and CO_2~~ N_2O, CO and CO_2 absorption lines. However, the spectral range includes another ~~N_2O line at 2227.843 cm^{-1}~~ N_2O line at 2227.843 cm^{-1}, which is slightly stronger than the other two (see ~~Fig.~~ Figure 5). Our approach is to fix the ~~mixing ratios~~ mole fractions of the first two ~~N_2O~~ N_2O lines to the stronger third one, in order to reduce the uncertainty ~~on retrieved N_2O~~ in retrieved N_2O and hence the noise on the ~~CO_2 and CO retrieval. The CO_2 absorption line originates from a molecular transition of the $^{13}C^{16}O_2$ carbon dioxide isotopologue, resulting in reduced accuracy if the isotopic composition of the sample is not accurately constrained. The~~ CO_2 and CO retrieval. The spectral baseline has been split into two parts, the first covering the first two ~~N_2O, CO_2 and CO~~ N_2O, CO_2 and CO lines, and the second covering the individual ~~N_2O~~ N_2O line only. Both are modeled as second-order polynomials.

3.1 Water vapor correction

In the current instrument setup, water vapor is not removed from sampled air before entering the sample cell. Therefore, the influence of water vapor on the retrieved ~~mixing ratios~~ mole fractions has to be corrected in order to report dry-air ~~mixing ratios~~mole fractions. Here, we correct for both, dilution and water broadening effects. The first describes the fact that concentrations appear smaller when analyzing moist air, although the dry air mole fraction might be constant. This effect can be remedied for if the absolute water concentration is known for each individual sample using Eq. 1

$$c_d = \frac{c_x}{(1 - c_{H_2O})} \tag{1}$$

where c_d is the dry-air mole fraction, c_x is the raw concentration of a particular species of interest diluted in moist air and c_{H_2O} is the water vapor concentration (Harazono et al., 2015). Spectroscopic water broadening effects are approximately an order of magnitude smaller than dilution effects, yet they do have to be corrected for to obtain precise measurements. HITRAN's air broadening parameters are listed for a particular chemical composition of air excluding water vapor. ~~H_2O~~H_2O, however, can be a more potent broadening agent than nitrogen or oxygen (Kooijmans et al., 2016). These coefficients have been determined using the setup depicted in ~~Fig.~~ Figure 6 and are summarized in ~~Tab.~~ Table 1. Therefore, the pressure broadening has to be modified to include this effect. Under dry air conditions it is common to split the pressure broadening into two parts: self-broadening and air-broadening. The self-broadening coefficient allows computation of the broadening induced by mutual collisions of a particular species of interest. The air-broadening coefficient can be used to approximate the broadening induced through collisions of a particular species with all the other species in a given air standard excluding the species itself. From the HITRAN definitions, the pressure-broadened half width at half maximum for a gas at pressure p and temperature T is given by

$$\gamma(p,T) = \left(\frac{T_{ref}}{T}\right)^{n_{air}} \left(\gamma_{air}\left(p - p_{self}\right) + \gamma_{self} p_{self}\right) \tag{2}$$

where T_{ref} is a fixed reference temperature (~~$T_{ref} = 296\,K$~~ $T_{ref} = 296$ K), p_{self} is the partial pressure of a particular species of interest and n_{air} is the coefficient of the temperature dependence of the air-broadened half width. This model has been extended to include collisions with ~~H_2O~~ H_2O molecules yielding

$$\gamma(p,T) = \left(\frac{T_{ref}}{T}\right)^{n_{air}} \left(\gamma_{air}\left(p - p_{self} - p_{H_2O}\right) + \gamma_{self} p_{self} + \gamma_{H_2O} p_{H_2O}\right) \tag{3}$$

with the partial pressure of water vapor p_{H_2O} and the water broadening coefficient γ_{H_2O}. The former can be computed from the measured water vapor concentration. The latter can be empirically determined. ~~Two~~ Not including the self and water foreign

Table 1. Empirically determined water vapor foreign broadening coefficients

Chemical species	~~CH_4~~ CH_4	~~C_2H_6~~ C_2H_6	~~CO_2~~ CO_2	~~CO~~ CO	~~N_2O~~ N_2O
Broadening coefficient $\times\gamma_{air}$	1.05	1.18	2.2	2.1	2.2

broadening leads to relative errors in the range of 0-2% for the described setup, depending on the species of interest. While small for C_2H_6 and CH_4 with $< 0.03\%$, the influence on retrieved CO is rather large with $\sim 2\%$. In order to obtain γ_{H_2O} two MFCs are used to ~~precisely modify mixing ratios~~ modify mole fractions of water vapor in a clean and dry calibration gas. ~~Theoretical computation of the water vapor mole fraction follows under the assumption that there is no water deposition on the enclosing flow channel surfaces and therefore the existence of a steady state flow condition. The amount of each constituent n in mols can be computed using the mass flow rate $\dot{m}$ (integrated over a suitable interval of time) and the corresponding molar mass M.~~ This does not involve measuring water vapor at absolute levels, instead it is only necessary to span the range of atmospheric H_2O. An additional downstream pump allows, in combination with a manually-controlled needle-valve, tuning the absolute pressure at the instrument inlet to simulate altitude changes. For these tests, the QCLS instrument has been operated at low flow rates of ~~approx. 1 $SLPM$~~ approximately 1 SLPM due to limitations on the two mass flow controllers. The water broadening coefficient γ_{H_2O} has been adjusted iteratively until reported dry-air mixing-ratios of the species of interest remained constant for the set of water vapor ~~mixing ratios~~mole fractions.

4 Ground-based performance

Extensive ground-based instrument checks have been conducted, including tests in a pressure chamber at the Karlsruhe Institute of Technology (KIT) and laboratory tests at DLR Oberpfaffenhofen, Germany. These tests confirmed the presence of an ambient pressure dependence found in earlier studies (i.e. Pitt et al. (2016)). Here, we show in-field, ground-based instrument

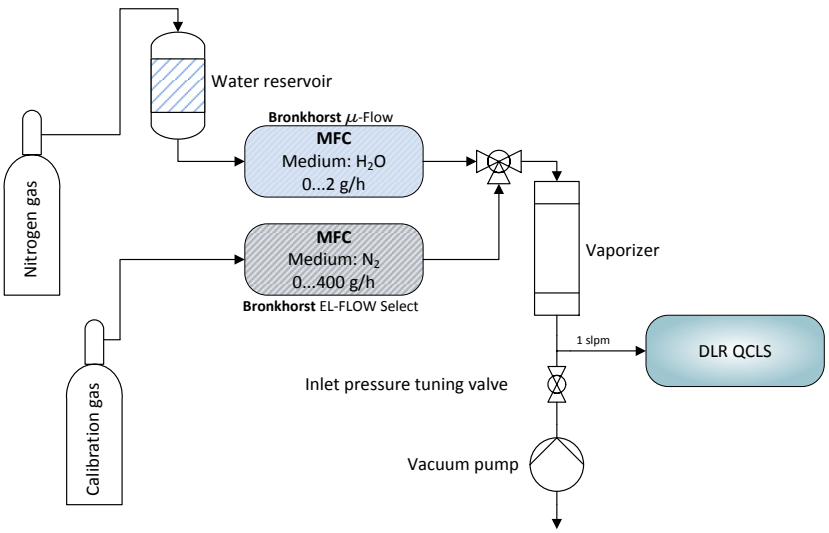

Figure 6. Schematic depicting the water correction lab setup. A reference gas can be humidified to typical atmospheric values between 0% and 2% absolute water using mass flow controllers and an electronically controlled vaporizer. A downstream pump allows for simulation of different flight levels.

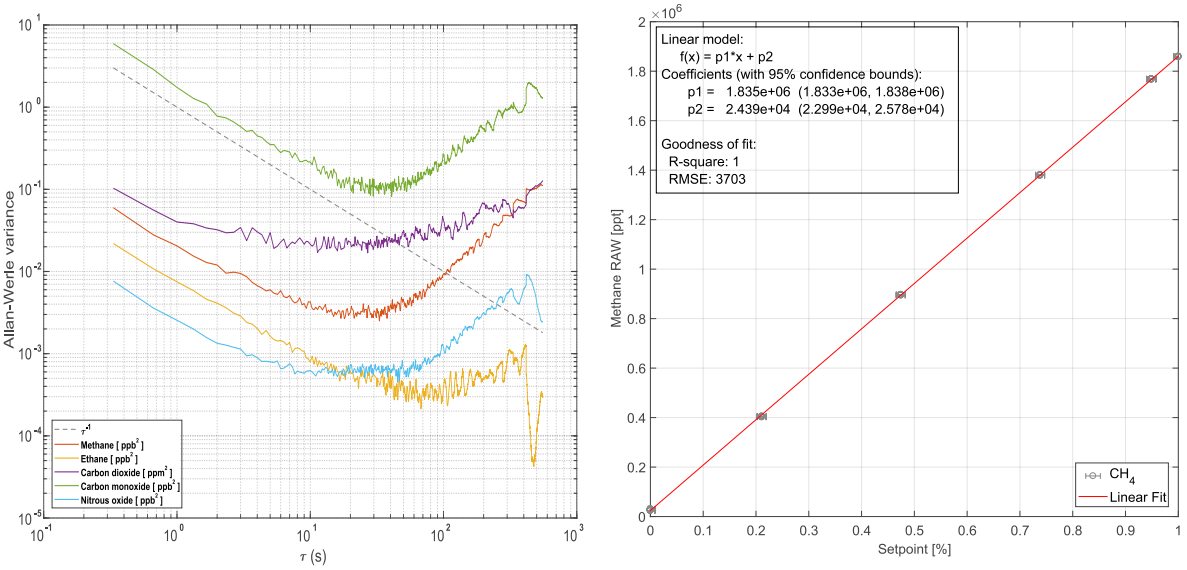

Figure 7. ~~Allan~~ Allan-Werle variance for all measured chemical species during ground-based operation (left panel). The right panel demonstrates linearity for methane is within achievable error bounds during ground-based operation using the online calibration gas mixing system from Section 2.3.

checks conducted in Hangar N-159 at NASA Wallops Flight Facility, Wallops Island, USA, to ensure proper instrument operation and determine instrument precision. Power drawn from the aircraft remained under ~~50 A~~ 50 A at all times and settled at approximately ~~40 A~~40 A. The volumetric flow rate stabilized at ~~23 $SLPM$~~ 23 SLPM for a sample cell pressure regulated at ~~50.0 $\pm$ 0.2 hPa (measured 1-sigma~~ 50.0 $\pm$ 0.5 hPa (0.2 hPa precision @ ~~5Hz, excluding absolute error~~5 Hz frequency). Typical precision (standard deviation for ~~1s~~ 1 s averaging) for ground-based operation is summarized in ~~Tab. 2. These values are in good agreement with the values reported by Aerodyne, Inc.. Achieved ground-based performance Chemical species H_2O CH_4 C_2H_6 CO_2 CO N_2O Precision $1s - 1\sigma$ 3.7 ppm 229 ppt 157 ppt 334 ppb 2.2 ppb 64 ppt~~ Table 2.

~~Fig.~~ Figure 7 shows the ~~Allan~~ Allan-Werle variance for common averaging times τ for the individual trace gases monitored. For most species averaging up to ~~20s~~ 20 s will decrease the signals standard deviation, before deteriorating effects (i.e. drift) occur. Figure 7 also addresses retrieved ~~mixing ratio~~ mole fraction linearity. Linearity checks have been carried out for all

Table 2. Typical $1s - 1\sigma$ precision during ground-based instrument checks.

Chemical species	H_2O	CH_4	C_2H_6	CO_2	CO	N_2O
Precision $1s - 1\sigma$	2.1 ppm	142 ppt	87 ppt	169 ppb	1.3 ppb	45 ppt

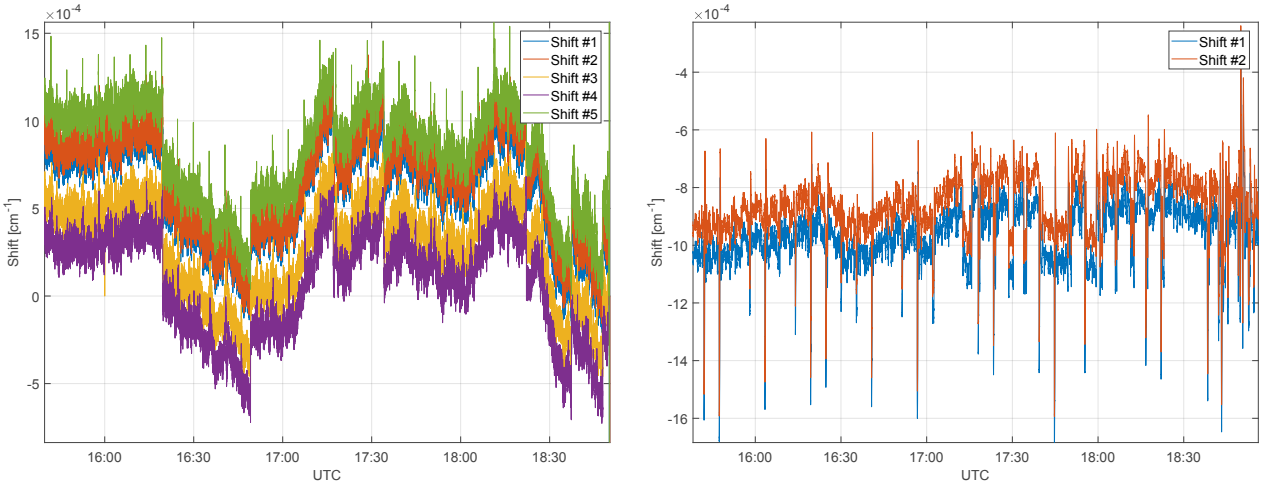

Figure 8. Spectral shifts for the CH_4-H_2O fit window (left) and the CO_2-CO-N_2O fit window (right). Spectral stability during ground-based operation is in the range of $\pm 10^{-3}$ cm^{-1}.

species using the calibration system described in Section 2.3. All retrieved species are linear within ~~error margin. CH_4~~ the achievable controlled mass flow uncertainties from Section 2.3. CH_4 is used in ~~Fig.~~ Figure 7 for demonstration purposes. Typical shift parameters (as introduced in Sect. 3) for ground-based operation are depicted in ~~Fig.~~ Figure 8 for the ~~CH_4-H_2O and CO_2-CO-N_2O micro~~ CH_4-H_2O and CO_2-CO-N_2O fit windows. These shift parameters can be considered as a tracer for instrument stability for both lasers. Overall spectral stability is in the range of ~~$\pm 10^{-3} cm^{-1}$~~ $\pm 10^{-3}$ cm^{-1}. Apart from expected low-frequency instability (due to thermal changes) on the lasers spectral output, high-frequency shifts are evident, including discontinuities. The source of these discontinuities remains unclear. They could be introduced by the software based frequency lock mechanism, by instabilities of the laser itself or by timing changes in the sampling. ~~The~~ Software based frequency lock refers to a controller regulating the laser temperature to compensate for drifts using the spectral shift as the controller input and the current to the Peltiers as controller output. The controller itself is implemented in software on the data analysis computer. The shape of the individual shifts match and so does their trend over time, which is a good indicator for a stable tuning rate during ground-based operation. ~~Spectral shifts for the CH_4-H_2O micro window (left) and the CO_2-CO-N_2O micro window (right). Spectral stability during ground-based operation is in the range of $\pm 10^{-3} cm^{-1}$.~~

5 Airborne instrument performance aboard NASA WFFs C-130

The instrument was successfully operated during 18 research flights aboard NASA Wallops Flight Facility's C-130 within the framework of the ACT-America fall 2017 field campaign. Other instrumentation in the ACT-America payload provided an excellent opportunity for instrument ~~intercomparison~~inter-comparison. In situ ~~CH_4, CO_2, and CO~~ CH_4, CO_2, and CO were measured using a PICARRO G2401-m cavity ring-down spectrometer, and in situ ~~CO_2, CH_4, and $H_2O(g)$~~ CO_2, CH_4, and

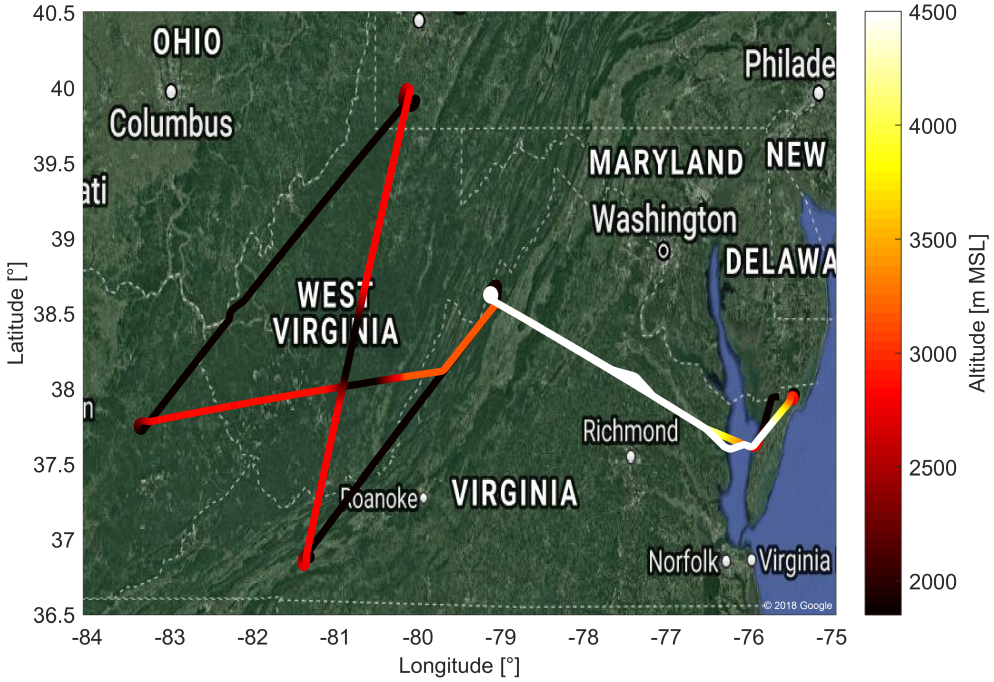

Figure 9. A typical flight during ACT-America. This figure shows the flight pattern for Oct. 3, 2017 with color coded altitude. The flight includes two low-altitude (≈ 300 m AGL) legs downwind and upwind of parts of the Marcellus shale area. High-altitude transects between the two low-altitude legs include two en route descents and ascents in West Virginia. Fair weather conditions and light southerly winds were present throughout the flight domain.

H_2O (g) were measured using a PICARRO G2301-m cavity ring-down analyzer. ~~Precise C_2H_6~~ Both PICARRO instruments are anchored to WMO X2007 for CO_2 (Zhao and Tans, 2006), WMO X2004A for CH_4 (Dlugokencky et al., 2005) and WMO X2014A for CO (Baer et al., 2002). Precise C_2H_6 measurements were obtained by periodic flask samples by NOAA ESRL. Three onboard lidars, and in situ sensors measuring the meteorological state variables - winds, temperature, pressure and water vapor - completed the C130s instrument suite. Here we present data from a typical flight (10/03/2017) to demonstrate the airborne instrument performance through inter-comparison with well-established measurement techniques: the cavity ring-down PICARRO greenhouse gas analyzers and flask samples.

As depicted in ~~Fig.~~ Figure 9, the flight starts off from the eastern U.S. (Wallops Flight Facility, Virginia). A high-altitude transect to West-Virginia is followed by two low-altitude legs downwind and upwind of parts of the Marcellus shale area: a large shale gas extraction region. The transects between the two low-altitude legs are flown at high altitude to facilitate nadir lidar observation, with two en route descents and ascents near the center. Figure 10 depicts dry-air ~~mixing ratios for CH_4, C_2H_6 and H_2O~~ mole fractions for CH_4, C_2H_6 and H_2O measured by the different instruments during the 5-hour flight. This figure provides evidence, that the QCLS ~~, PICARRO and flask methane data are in good agreement~~ and PICARRO methane

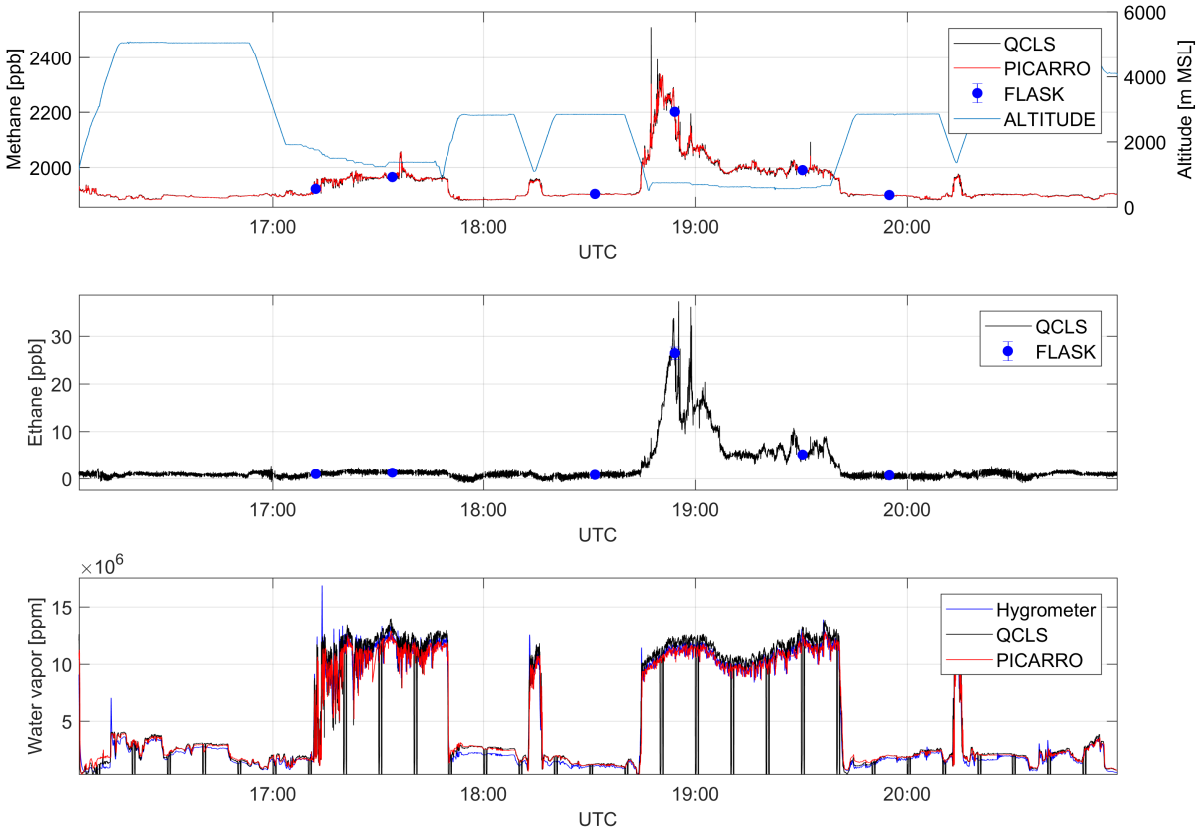

Figure 10. A ~~typical fair-weather flight during ACT-America. This figure shows the flight pattern~~ direct comparison between dry-air mole fractions retrieved from different measurement techniques for a complete flight on Oct. 3, ~~2017 with color-coded altitude~~2017. Depicted are methane (uppermost panel), ethane (center panel) and water vapor (lowermost panel) mole fractions. ~~The flight includes two low-altitude~~ QCLS-retrieved methane data matches with PICARRO and flask data to within 1.4 ppb ($\approx$ ~~1000 $ft\,AGL$~~ 1σ) ~~legs downwind~~ and ~~upwind of parts of the Marcellus shale area~~3.9 ppb (1σ), respectively, after correcting for a constant bias. ~~High-altitude transects between~~ QCLS-retrieved ethane data agrees with flask data to within 0.4 ppb (1σ). Water vapor sensed by an on-board dewpoint hygrometer does differ from the ~~two low-altitude legs include two en route descents~~ PICARRO and ~~ascents in West Virginia~~QCLS data.

data agree to within 1.4 ppb (1σ) over the entire flight. QCLS and flask methane data agree to within 3.9 ppb (1σ). It should be noted, that care must be taken when interpreting the differences between slow flask samples and fast in situ measurements for high-variability flight segments. The center panel of ~~Fig.~~ Figure 10 depicts the QCLS-retrieved ~~C_2H_6~~ C_2H_6 data superimposed with flask measurements. Here the QCLS-retrieved ethane data ~~also~~ matches the flask measurements (blue dots) ~~within error margin~~to within 0.4 ppb (1σ). Unlike the QCLS, PICARRO and flask data are both sampled through an upstream dryer. These were computed by interpolating QCLS data to the flask end fill times. The lowermost panel of ~~Fig.~~ Figure 10 provides water vapor ~~mixing ratios~~ mole fractions obtained from an ~~onboard~~ on-board dewpoint hygrometer, from the G2301-m PICARRO analyzer and from the QCLS. The QCLS water vapor data is used to correct for water vapor effects during the retrieval of

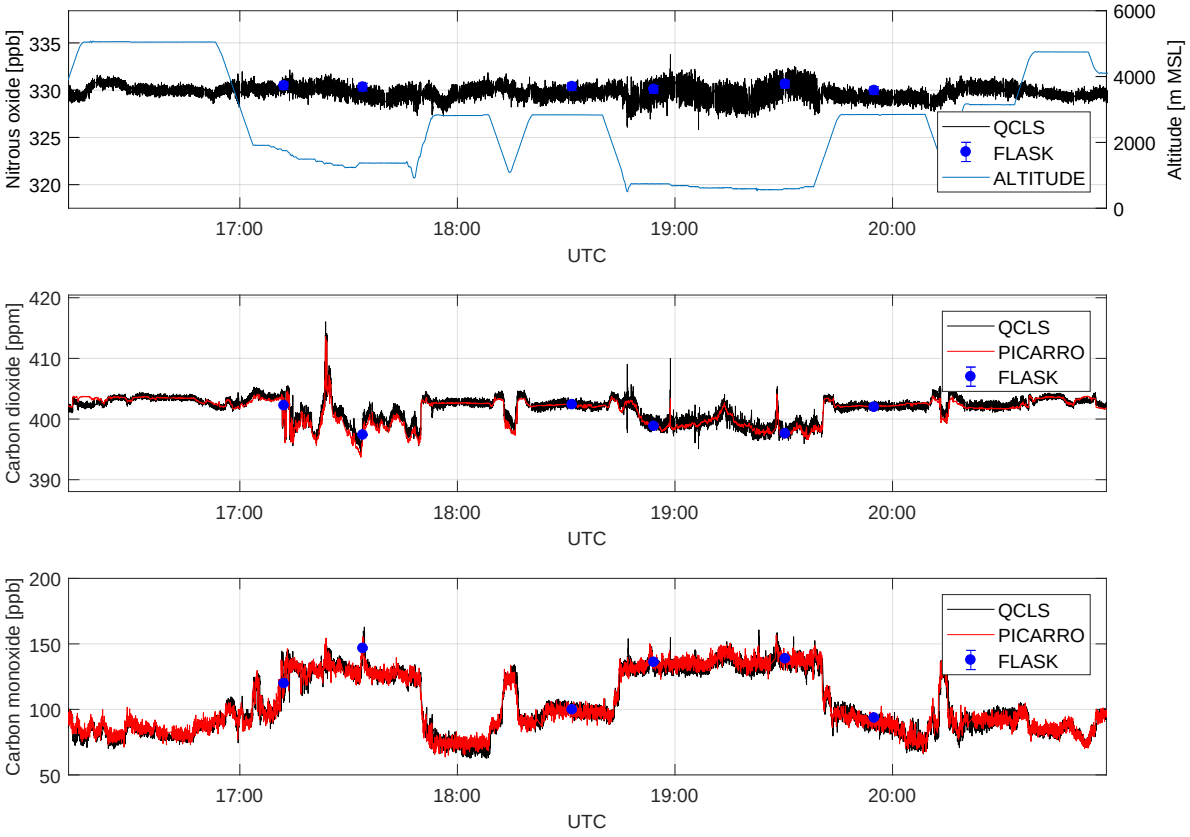

Figure 11. ~~A direct comparison between dry-air mixing ratios~~ Dry-air mole fractions retrieved from different measurement techniques for a complete flight on Oct. 3, 2017. Depicted are ~~methane~~ nitrous oxide (uppermost panel), ~~ethane~~ carbon dioxide (center panel) and ~~water vapor~~ carbon monoxide (lowermost panel) ~~mixing ratios~~mole fractions.~~QCLS-retrieved methane data is in good accordance with PICARRO and flask data. QCLS-retrieved ethane data is in good agreement with flask data too. Water vapor sensed by an onboard hygrometer does differ from the PICARRO and QCLS data.~~

dry-air ~~mixing ratios~~ mole fractions from the QCLS raw spectra as described in Sect. 3.1. By taking a closer look on the upper two panels, the benefit of simultaneously measuring several species can be readily identified. Figure 10 shows enhanced ~~CH_4 without coinciding C_2H_6~~ CH_4 without coinciding C_2H_6 enhancements for the first low-altitude leg. For the second low-altitude leg above the Marcellus area, however, concurrent ~~CH_4 and C_2H_6 enhancements suggest natural gas being the dominating~~ CH_4 and C_2H_6 enhancements suggest that natural gas is the dominant source.

~~Dry-air mixing ratios retrieved from different measurement techniques for a complete flight on Oct. 3, 2017. Depicted are nitrous oxide (uppermost panel), carbon dioxide (center panel) and carbon monoxide (lowermost panel) mixing ratios.~~ Time series for the species ~~N_2O, CO and CO_2~~ N_2O, CO and CO_2 are shown in ~~Fig. 11. A good overall match between the different data sources can be identified. The N_2O~~ Figure 11. The data obtained are comparable within instrument uncertainties. The N_2O time series matches available flask data to within ~~± 1 ppb. The CO_2~~ $\pm$1.1 ppb. The CO_2 absorption is retrieved from a molecular

transition of the ~~$^{13}C^{16}O_2$~~ $^{13}C^{16}O_2$ carbon dioxide isotopologue and scaled with its natural abundance of approximately 1.1 % (Gordon et al., 2017)) to report total ~~CO_2~~ CO_2. Despite the much lower abundance compared to ~~$^{12}C^{16}O_2$~~ $^{12}C^{16}O_2$ the QCLS-retrieved ~~CO_2~~ CO_2 data coincides with PICARRO data to within ~~$\pm 2 ppm (1\sigma)$~~ ± 0.6 ppm (1σ) after correcting for a constant bias (see below). QCLS-retrieved ~~CO mixing ratios~~ CO mole fractions (center panel) agree with PICARRO-retrieved data to within ~~$\pm 5 ppb (1\sigma)$. Fig.~~ ± 5 ppb (1σ). Figure 11 suggests that in-flight precision depends on whether flying within the planetary boundary layer or above it. This is due to aircraft vibration excited by running engines and turbulence propagating into the instrument optics inducing slight changes in optical alignment ~~.~~ and enhanced natural variability in the planetary boundary layer. We identified temperature fluctuations within ~ 0.3 K, pressure changes of up to ~ 200 hPa and relative humidity changes of up to 35 % in the instruments optical compartment during this flight. ~~The left panel shows the cabin~~

Table 3. Typical in-flight performance including contributions to overall uncertainty. The total measurement uncertainty at ~~1s~~ 1 s temporal resolution is given by the quadrature sum of the individual contributors. Due to the lack of the appropriate NOAA standards during the deployment, the uncertainties in C_2H_6, CO and N_2O include combined uncertainties from concurrently measuring instruments (CRDS & Flasks). The total uncertainties stated for these species do therefore not reflect the intrinsic uncertainties of the instrument, but worst-case values, that may be better given the availability of appropriate standards. The WMO compatibility goals for Global Atmosphere Watch network compatibility among laboratories and central facilities have been added for completeness.

Chemical species	~~H_2O~~ H_2O	~~CH_4~~ CH_4	~~C_2H_6~~ C_2H_6	~~CO_2~~ CO_2	~~CO~~ CO	~~N_2O~~ N_2O
Precision $1s - 1\sigma$ (within PBL)	16.2 ppm	740 ppt	205 ppt	460 ppb	2.2 ppb	439 ppt
Precision $1s - 1\sigma$ (above PBL)	2.5 ppm	300 ppt	146 ppt	182 ppb	1.4 ppb	208 ppt
Working standard reproducibility (1σ)	—	0.03 ppb	—	0.1 ppm	—	—
Compared instrument uncertainty (1σ)	—	—	1.5 ppb	—	5.0 ppb	0.4 ppb
Measurement calibration (1σ)	—	~~2.0~~1.5 ppb	0.5 ppb	0.9 ppm	~~5.0~~4.4 ppb	0.5 ppb
H_2O correction (1σ)	—	0.8 ppb	0.1 ppb	0.2 ppm	0.2 ppb	0.1 ppb
WMO compatibility goal	—	2.0 ppb	—	0.1 ppm	2.0 ppb	0.1 ppb
~~Total~~ Total 1s-1σ uncertainty	—	~~2.3~~1.85 ppb	1.6 ppb	1.0 ppm	~~7.4~~7.0 ppb	0.8 ppb

~~pressure dependence for a typical flight on Oct. 3, 2017. The large cabin pressure dependence in excess of $0.3 ppb hPa^{-1}$ reported by Pitt et al. (2016) could not be reproduced. The right hand side panel shows a temporal zoom on the methane data at 18:47 UTC to emphasize the benefit of high-frequency measurements.~~

Typical in-flight precision figures based on ambient measurements at stable conditions for both regimes (standard deviation for 1s averaging) are summarized in ~~Tab.~~ Table 3. Total measurement uncertainty can be estimated from the uncertainty ~~on~~ of the working standards, the uncertainty ~~on~~ of calibration sequence evaluation, the uncertainty introduced by the H_2O correction, the precision of the instrument and errors due to drift. ~~The relative error on the NOAA standards is stated with 0.2 %, which expands to $\sim 0.2 ppm$ and $\sim 3.6 ppb$ for our CO_2 and CH_4 standard respectively.~~ We found a bias constant for the whole measurement series of ~~$\sim 2 ppb$ for CH_4 and $\sim 10 ppm$ for CO_2~~ ~ 2 ppb for CH_4 and ~ 10 ppm for CO_2 between the QCLS

and PICARRO/FLASK datasets. This constant bias has been corrected for. The ~~large CO_2 bias most possibly results from a difference in the~~ origin of the biases is not yet fully understood. It was suggested that water vapor correction could have an impact on this. The reason for this assumption is that the calibration standards are always dry, whereas sampled air is not dried before entering the sample cell. Correlation plots however show no signficant influence of water vapor on the residuals between the dry-air-sampling Picarro and the QCLS. It is therefore very unlikely that the water vapor correction is the source of the large bias in CO_2. Instead we identified the difference in isotopic composition of the calibration standard ~~relative to the sampled air~~versus sampled atmospheric air as the most probable cause. In this study we used working standards of synthetic nature from *Air Liquide*. Usually these are produced with CO_2 from natural gas & oil combustion processes. We determined the CH_4 and CO_2 values of each working standard gas cylinder using a NOAA-anchored (Cert.-Nr. CB11361) Picarro G-1301m. This has the drawback that we do not know the isotopic composition of our working standards as its impact had been considered negligible, e.g. Chen et al. (2010). We learned during development of JFIT, that the instrument is using a $^{13}C^{16}O_2$ line to derive ambient CO_2. We estimate the required isotopic composition that could explain a large bias of up to 17 ppm (see Supplement Section 3) in CO_2 to be 98.447% primary isotopologue and 1.079% secondary isotopologue or $\delta^{13}C = -19.6$ ‰ which seems reasonable according to B. Coplen et al. (2002). Since we are reporting retrieved ~~mixing ratios~~ mole fractions relative to the WMO scale, ~~however,~~ only the working standard reproducibility contributes to the total uncertainty ~~. Uncertainty on~~ of CH_4. Comparability of CO_2 is difficult to assess here because of the unknown isotopic composition in our working standards. Uncertainty in the other measured species is taken from the ACT-America dataset to allow for WMO traceability. ~~The uncertainty on~~ Due to the lack of the appropriate NOAA standards during the deployment, the uncertainties in C_2H_6, CO and N_2O include uncertainties reported in the ACT-America dataset from concurrently measuring instruments (CRDS & Flasks). The total uncertainties stated for these species do therefore not reflect the intrinsic uncertainties of the instrument, but worst-case values, that may be better given the availability of appropriate standards in future deployments. The uncertainty of calibration sequence evaluation (see 2.3) is estimated with the double of the measurement precision and the uncertainty introduced by the ~~H_2O~~ H_2O correction is estimated from Eq. 1 using an assumed relative error on retrieved water vapor of 2%. Errors originating from instrument drift are considered negligible due to our frequent calibration strategy (see Section 2.3). The total uncertainty is given by the quadrature sum of the individual contributors, listed in ~~Tab. 3.~~ Table 3. Table 3 further includes the WMO compatibility goals for Global Atmosphere Watch (GAW) network compatibility among laboratories and central facilities. Precision (uncertainty) figures given in Table 3 can be compared to 2s-1σ PICARRO G2401-m airborne precision (uncertainty) estimates based on ambient measurements at stable conditions of 0.3 (2) ppb, 0.02 (0.1) ppm and 2.0 (5) ppb for CH_4, CO_2 and CO, respectively.

A severe cabin pressure dependence in excess of ~~$0.3 ppb hPa^{-1}$ in CH_4 mixing ratio~~ 0.3 ppb hPa^{-1} in CH_4 mole fraction has been previously reported for airborne ~~Aerodyne~~ TILDAS instrumentation (Pitt et al., 2016). ~~We were not able to reproduce this large cabin pressure dependence~~ This instrumentation however physically differs from the one reported in this study. It is not possible to accurately compare the dependencies of one instrument relative to another since many factors/quantities involved are instrument-specific, e.g. the open-path length, the positioning and properties of optical elements, like windows, mirrors, etc., the stiffness and thermal expansion coefficient of the employed optical stands. We were nevertheless able to effectively

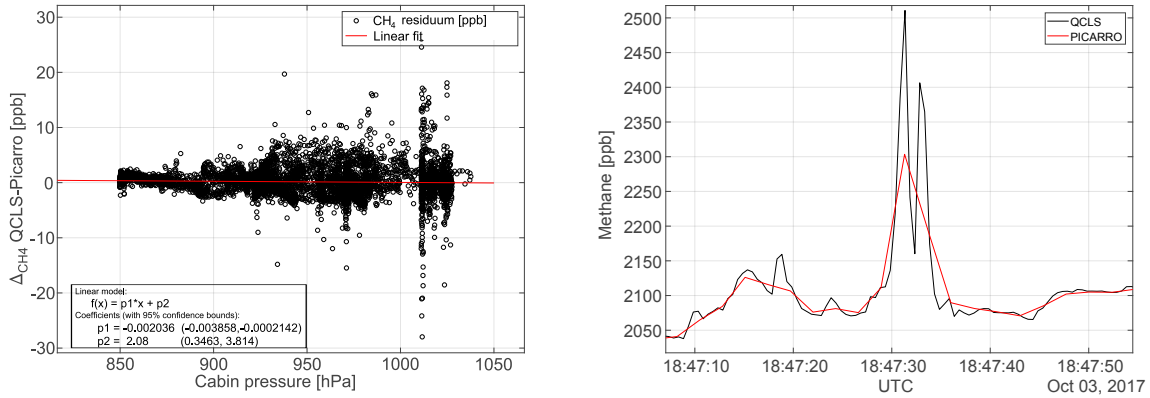

Figure 12. The left panel shows the cabin pressure dependence for a typical flight on Oct. 3, 2017. The large cabin pressure dependence in excess of $0.3\,ppb$ hPa^{-1} reported by Pitt et al. (2016) has effectively been minimized using the calibration strategy from Sect. 2.3. The right hand side panel shows a temporal zoom on the CH_4 mole fractions at 18:47 UTC to emphasize the benefit of high-frequency measurements.

minimize cabin pressure dependencies during operation of the QCLS instrument aboard the C130 using the calibration strategy from Sect. 2.3. This required a total calibration gas amount of ~ 3.5 m^3 (excluding zero air) for the 18 research flights. Figure 12 (left panel) shows the difference in ~~CH_4~~ CH_4 dry-air ~~mixing ratio~~ mole fraction reported by the QCLS and the PICARRO instrument as a function of cabin pressure during the research flight described above. The large scatter results from different sampling patterns among the two instruments, hindering a one-to-one comparison of the QCLS measurements with the PICARRO. While the QCLS samples continuously with a frequency of ~~$2\,Hz$~~ ~~(1.5 kHz~~ 2 Hz (1.5 kHz sweep frequency), the PICARRO samples with a frequency of ~~$0.5\,Hz$~~ 0.5 Hz one species after the other. For ~~CH_4~~CH_4, for example, the PICARRO uses the first ~~$0.5\,s$ of the $2\,s$~~ 0.5 s of the 2 s sampling time, implying that, for the later ~~$1.5\,s$~~1.5 s, the PICARRO is insensitive to ~~CH_4~~CH_4. Therefore, it is difficult to mimic the PICARRO sampling by averaging the QCLS data as it would be required for a one-to-one comparison. Instead we decided to linearly interpolate QCLS data to the PICARRO timescale. The fast response time of the QCLS instrument allows for better sampling of spatially narrow plumes, as can be seen from the right hand side panel in ~~Fig.~~ Figure 12. This panel zooms in on a relevant portion of the methane data from ~~Fig.~~ Figure 10 and demonstrates that two mutually-separated plumes can be identified from the high frequency QCLS data at 18:47 UTC, where only a single enhancement can be seen from PICARRO data. Furthermore, absolute enhancement and area beneath the peak(s) differ for the two instruments, due to the different sampling patterns. Figure 13 compares the QCLS ~~mixing ratios~~ mole fractions to the PICARRO instrument and to the flask samples after correcting for a bias constant for the whole measurement series. The upper panels show differences in retrieved ~~mixing ratios~~ mole fractions between the QCLS and the cavity ring-down instrument for the flight on Oct. 3, 2017, exhibiting a near normal distribution. This hints towards residuals originating from random processes, i.e. noise. Despite the different sampling time and pattern, the measurements exhibit a compatibility to the calibrated cavity ring-down observations of 1.4 ppb in CH_4, 0.6 ppm in CO_2 and 5.0 ppb in CO. Although interpretation of the differences to

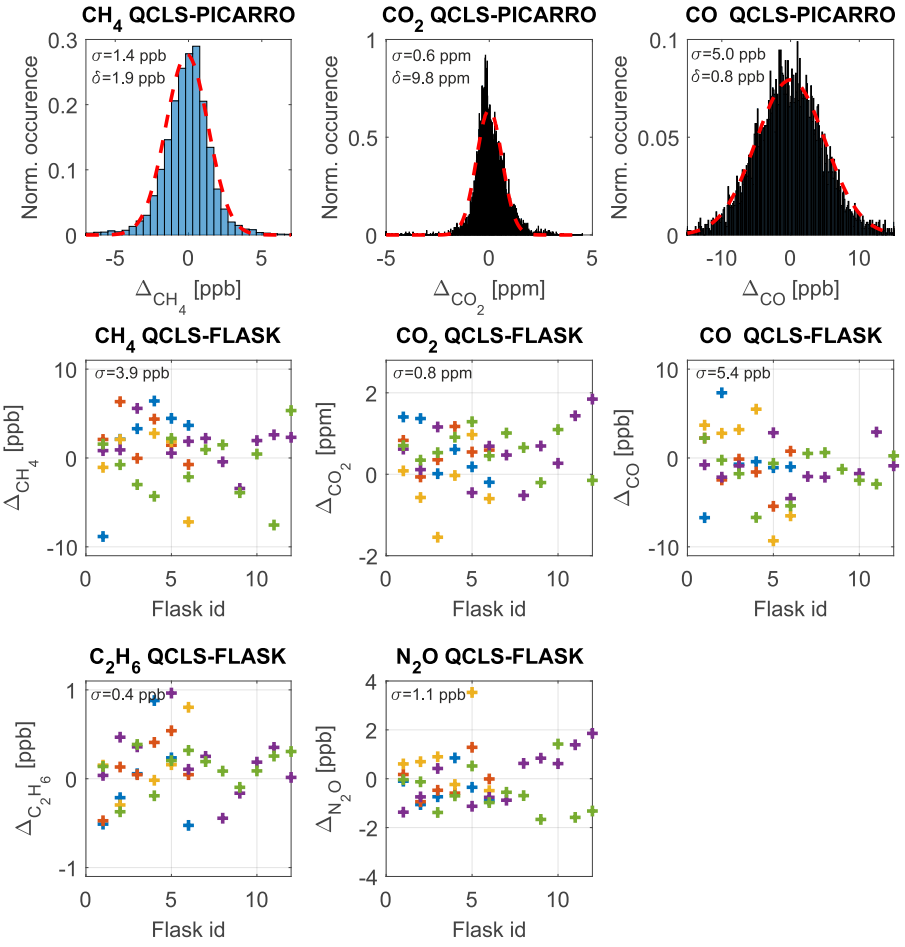

Figure 13. Comparison of QCLS derived ~~mixing ratios~~ mole fractions to well-established in-flight PICARRO data and flask samples after correcting for a bias (δ) constant for the whole measurement series including standard deviations σ. Interpretation of the errors against flask samples is difficult for high-variability flight segments, due to the large flask sampling time. The residual plots show color-coded data from 5 typical flights on 10/03/2017, 10/11/2017, 10/14/2017, 10/18/2017 and 10/20/2017.

flask samples is difficult for high-variability flight segments, the lower panels of ~~Fig.~~ Figure 13 show a good agreement for five typical flights (10/03/2017, 10/11/2017, 10/14/2017, 10/18/2017, 10/20/2017) during the ACT-America campaign.

6 Conclusions

We adapted the commercially-available QCL/ICL based *Dual Laser Trace Gas Monitor* from *AERODYNE RESEARCH INC., Billerica, USA* for airborne ~~operation~~ flux estimation (e.g. via the mass-balance approach) and demonstrate successful operation ~~over 18~~ for representative research flights aboard NASA Wallops Flight Facility's C-130 during the ACT-America field

campaign in fall 2017. Known cabin-pressure dependencies (Gvakharia et al. (2018); Pitt et al. (2016)) on the retrieved ~~mixing ratios~~ mole fractions are effectively minimized using a frequent (5 to 10mins interval) two-point calibration approach obtained by flushing the sample cell with "zero" and "target" gases. This allows for a measurement duty cycle of $\geq 90\,\%$ when operating at sample flow rates near ~~23 $SLPM$~~23 SLPM. A custom retrieval software has been developed to ~~allow for independent processing of raw spectra. We minimize retrieval artifacts by introducing a new way to handle spectral shifts. We reduce fitting residuals by implementing open path water vapor absorption using an auxiliary sensor mounted inside the instruments optics compartment.~~ learn about possible error sources, mitigation possibilities of instrument dependencies and to be able to extend the instruments capabilities in the future. Apart from low frequency laser instability we identify high frequency "jumps" on the spectral axis, possibly due to the instruments frequency lock mechanism. In-flight performance has been assessed using data obtained during the research flight on the 3rd Oct. 2017 above the eastern U.S.. We identify two precision regimes whether flying within the planetary boundary layer or above, due to aircraft vibration propagating into the instrument optics and related slight changes in optical alignment. Typical in-flight precision figures for boundary layer flights (standard deviation for 1s averaging) are ~~740 ppt, 205 ppt, 460 ppb, 2.2 ppb, 137 ppt, 16 ppm for CH_4, C_2H_6, CO_2, CO, N_2O and H_2O~~ 740 ppt, 205 ppt, 460 ppb, 2.2 ppb, 137 ppt, 16 ppm for CH_4, C_2H_6, CO_2, CO, N_2O and H_2O respectively. Precision figures improve to approximately the half for flights above the PBL. We estimate a total measurement uncertainty of ~~2.3 ppb, 1.6 ppb, 1.0 ppm, 7.4 ppb and 0.8 ppb in CH_4, C_2H_6, CO_2, CO and N_2O~~1.85 ppb, 1.6 ppb, 1.0 ppm, 7.0 ppb and 0.8 ppb in CH_4, C_2H_6, CO_2, CO and N_2O, respectively. We demonstrate ~~an excellent agreement~~ QCLS comparisons to concurrent flask sample and cavity-ringdown measurements within combined measurement uncertainty for all targeted species. The instrument retrieves carbon dioxide ~~mixing ratios via a $^{13}C^{16}O_2$ absorption lineand is thus shown to be capable of detecting isotopologue level mixing ratios, which will be picked up in the near future to modify the instrument for airborne isotope ratio analysis~~mole fractions via a $^{13}C^{16}O_2$ absorption line. We find that precise knowledge of the $\delta^{13}C$ of the working standards and the sampled air is needed to enhance CO_2 compatibility when operating on the 2227.604 cm^{-1} $^{13}C^{16}O_2$ absorption line.

Code and data availability. Software code and data are available from the authors upon request.

Competing interests. The authors are not aware of any competing interests.

Acknowledgements. We thank DLR VO-R for funding the young investigator research group "Greenhouse Gases". We also acknowledge funding from BMBF under project "AIRSPACE" (Grant-no. FKZ01LK170). The Atmospheric Carbon and Transport (ACT) - America project is a NASA Earth Venture Suborbital 2 project funded by NASA's Earth Science Division (Grant NNX15AG76G to Penn State). Aircraft operations and U.S. investigators were funded via the ACT-America project. We greatly appreciate continuous support from Hans Schlager and Markus Rapp from DLR. We further thank the GLORIA team, especially Christof Piesch and Hans Nordmeyer at the Karlsruhe Institute of Technology (KIT) for enabling us pressure testing the rack-mounted QCLS in a climate chamber. We also thank Paul Stock and Monika Scheibe from DLR and Martin Nowicki from NASA WFF for engineering support. Furthermore we would like to thank everyone involved during the ACT-America field campaigns for their relentless dedication and the helpful discussions, especially Alan Fried, Bing Lin, John Nowak, Linda D. Thompson, Charles E. Juenger. A special thanks to Mark Zahniser and Dave Nelson from Aerodyne Inc. for their valuable support whenever help was needed.

References

Abrarov, S. and Quine, B.: A Rational Approximation for Efficient Computation of the Voigt Function in Quantitative Spectroscopy, 7, 2015.

B. Coplen, T., Bohlke, J., De Bièvre, P., Ding, T., Holden, N., Hopple, J., R. Krouse, H., Lamberty, A., S. Peiser, H., Révész, K., E. Rieder, S., and J. R. Rosman, K.: Isotope-abundance Variations of Selected Elements (IUPAC Technical Report), Pure and Applied Chemistry - PURE APPL CHEM, 74, 1987–2017, https://doi.org/10.1351/pac200274101987, 2002.

Baer, D., Paul, J., Gupta, M., and O'Keefe, A.: Sensitive absorption measurements in the near-infrared region using off-axis integrated-cavity-output spectroscopy, Applied Physics B, 75, 261–265, https://doi.org/10.1007/s00340-002-0971-z, https://doi.org/10.1007/s00340-002-0971-z, 2002.

Barkley, Z. R., Lauvaux, T., Davis, K. J., Deng, A., Miles, N. L., Richardson, S. J., Cao, Y., Sweeney, C., Karion, A., Smith, M., Kort, E. A., Schwietzke, S., Murphy, T., Cervone, G., Martins, D., and Maasakkers, J. D.: Quantifying methane emissions from natural gas production in north-eastern Pennsylvania, Atmospheric Chemistry and Physics, 17, 13 941–13 966, https://doi.org/10.5194/acp-17-13941-2017, https://www.atmos-chem-phys.net/17/13941/2017/, 2017.

Beck, M., Hofstetter, D., Aellen, T., Faist, J., Oesterle, U., Ilegems, M., Gini, E., and Melchior, H.: Continuous Wave Operation of a Mid-Infrared Semiconductor Laser at Room Temperature, Science, 295, 301–305, https://doi.org/10.1126/science.1066408, http://science.sciencemag.org/content/295/5553/301, 2002.

Capasso, F.: High-performance midinfrared quantum cascade lasers, 49, 1102–, 2010.

Catoire, V., Robert, C., Chartier, M., Jacquet, P., Guimbaud, C., and Krysztofiak, G.: The SPIRIT airborne instrument: a three-channel infrared absorption spectrometer with quantum cascade lasers for in situ atmospheric trace-gas measurements, Applied Physics B, 123, 244, https://doi.org/10.1007/s00340-017-6820-x, https://doi.org/10.1007/s00340-017-6820-x, 2017.

Chen, H., Winderlich, J., Gerbig, C., Hoefer, A., Rella, C. W., Crosson, E. R., Van Pelt, A. D., Steinbach, J., Kolle, O., Beck, V., Daube, B. C., Gottlieb, E. W., Chow, V. Y., Santoni, G. W., and Wofsy, S. C.: High-accuracy continuous airborne measurements of greenhouse gases (CO_2 and CH_4) using the cavity ring-down spectroscopy (CRDS) technique, Atmospheric Measurement Techniques, 3, 375–386, https://doi.org/10.5194/amt-3-375-2010, https://www.atmos-meas-tech.net/3/375/2010/, 2010.

Ciais, P., Sabine, C., Bala, G., Bopp, L., Brovkin, V., Canadell, J., Chhabra, A., DeFries, R., Galloway, J., Heimann, M., Jones, C., Le Quéré, C., Myneni, R., Piao, S., and Thornton, P.: Carbon and Other Biogeochemical Cycles, book section 6, p. 465–570, Cambridge University Press, Cambridge, United Kingdom and New York, NY, USA, https://doi.org/10.1017/CBO9781107415324.015, www.climatechange2013.org, 2013.

Dlugokencky, E. J., Myers, R. C., Lang, P. M., Masarie, K. A., Crotwell, A. M., Thoning, K. W., Hall, B. D., Elkins, J. W., and Steele, L. P.: Conversion of NOAA atmospheric dry air CH4 mole fractions to a gravimetrically prepared standard scale, Journal of Geophysical Research: Atmospheres, 110, https://doi.org/10.1029/2005JD006035, https://agupubs.onlinelibrary.wiley.com/doi/abs/10.1029/2005JD006035, 2005.

Filges, A., Gerbig, C., Chen, H., Franke, H., Klaus, C., and Jordan, A.: The IAGOS-core greenhouse gas package: a measurement system for continuous airborne observations of CO2, CH4, H2O and CO, Tellus B: Chemical and Physical Meteorology, 67, 27 989, https://doi.org/10.3402/tellusb.v67.27989, https://doi.org/10.3402/tellusb.v67.27989, 2015.

Fried, A. and Richter, D.: Infrared Absorption Spectroscopy, chap. 2, pp. 72–146, John Wiley & Sons, Ltd, https://doi.org/10.1002/9780470988510.ch2, https://onlinelibrary.wiley.com/doi/abs/10.1002/9780470988510.ch2, 2007.

Gordon, I., Rothman, L., Hill, C., Kochanov, R., Tan, Y., Bernath, P., Birk, M., Boudon, V., Campargue, A., Chance, K., Drouin, B., Flaud, J.-M., Gamache, R., Hodges, J., Jacquemart, D., Perevalov, V., Perrin, A., Shine, K., Smith, M.-A., Tennyson, J., Toon, G., Tran, H., Tyuterev, V., Barbe, A., Császár, A., Devi, V., Furtenbacher, T., Harrison, J., Hartmann, J.-M., Jolly, A., Johnson, T., Karman, T., Kleiner, I., Kyuberis, A., Loos, J., Lyulin, O., Massie, S., Mikhailenko, S., Moazzen-Ahmadi, N., Müller, H., Naumenko, O., Nikitin, A., Polyansky, O., Rey, M., Rotger, M., Sharpe, S., Sung, K., Starikova, E., Tashkun, S., Auwera, J. V., Wagner, G., Wilzewski, J., Wcisło, P., Yu, S., and Zak, E.: The HITRAN2016 molecular spectroscopic database, Journal of Quantitative Spectroscopy and Radiative Transfer, 203, 3 – 69, https://doi.org/https://doi.org/10.1016/j.jqsrt.2017.06.038, http://www.sciencedirect.com/science/article/pii/S0022407317301073, hITRAN2016 Special Issue, 2017.

Gvakharia, A., Kort, E. A., Smith, M. L., and Conley, S.: Testing and evaluation of a new airborne system for continuous N_2O, CO_2, CO, and H_2O measurements: the Frequent Calibration High-performance Airborne Observation System (FCHAOS), Atmospheric Measurement Techniques Discussions, 2018, 1–22, https://doi.org/10.5194/amt-2018-201, https://www.atmos-meas-tech-discuss.net/amt-2018-201/, 2018.

Harazono, Y., Iwata, H., Sakabe, A., Ueyama, M., Takahashi, K., Nagano, H., Nakai, T., and Kosugi, Y.: Effects of water vapor dilution on trace gas flux, and practical correction methods, Journal of Agricultural Meteorology, 71, 65–76, https://doi.org/10.2480/agrmet.D-14-00003, 2015.

Harrison, J. J., Allen, N. D., and Bernath, P. F.: Infrared absorption cross sections for ethane (C2H6) in the $3\mu m$ region, Journal of Quantitative Spectroscopy and Radiative Transfer, 111, 357 – 363, https://doi.org/https://doi.org/10.1016/j.jqsrt.2009.09.010, http://www.sciencedirect.com/science/article/pii/S0022407309002866, 2010.

IPCC, .: Climate Change 2014: Synthesis Report. Contribution of Working Groups I, II and III to the Fifth Assessment Report of the Intergovernmental Panel on Climate Change [Core Writing Team, R.K. Pachauri and L.A. Meyer (eds.)], IPCC, Geneva, Switzerland, 2014.

Kim, M., Bewley, W. W., Canedy, C. L., Kim, C. S., Merritt, C. D., Abell, J., Vurgaftman, I., and Meyer, J. R.: High-power continuous-wave interband cascade lasers with 10 active stages, Opt. Express, 23, 9664–9672, https://doi.org/10.1364/OE.23.009664, http://www.opticsexpress.org/abstract.cfm?URI=oe-23-8-9664, 2015.

Klemm, O., Hahn, M. K., and Giehl, H.: Airborne, Continuous Measurement of Carbon Monoxide in the Lower Troposphere, Environmental Science & Technology, 30, 115–120, https://doi.org/10.1021/es950145j, https://doi.org/10.1021/es950145j, 1996.

Kooijmans, L. M. J., Uitslag, N. A. M., Zahniser, M. S., Nelson, D. D., Montzka, S. A., and Chen, H.: Continuous and high-precision atmospheric concentration measurements of COS, CO_2, CO and H_2O using a quantum cascade laser spectrometer (QCLS), Atmospheric Measurement Techniques, 9, 5293–5314, https://doi.org/10.5194/amt-9-5293-2016, https://www.atmos-meas-tech.net/9/5293/2016/, 2016.

Marquardt, D.: An Algorithm for Least-Squares Estimation of Nonlinear Parameters, Journal of the Society for Industrial and Applied Mathematics, 11, 431–441, https://doi.org/10.1137/0111030, https://doi.org/10.1137/0111030, 1963.

McManus, J. B., Zahniser, M. S., and Nelson, D. D.: Dual quantum cascade laser trace gas instrument with astigmatic Herriott cell at high pass number, Appl. Opt., 50, A74–A85, https://doi.org/10.1364/AO.50.000A74, http://ao.osa.org/abstract.cfm?URI=ao-50-4-A74, 2011.

McManus, J. B., Nelson, D. D., and Zahniser, M. S.: Design and performance of a dual-laser instrument for multiple isotopologues of carbon dioxide and water, Opt. Express, 23, 6569–6586, https://doi.org/10.1364/OE.23.006569, http://www.opticsexpress.org/abstract.cfm?URI=oe-23-5-6569, 2015.

O. L. Cambaliza, M., Shepson, P., Bogner, J., R. Caulton, D., Stirm, B., Sweeney, C., A. Montzka, S., Gurney, K., Spokas, K., Salmon, O., Lavoie, T., Hendricks, A., Mays, K., Turnbull, J., R. Miller, B., Lauvaux, T., Davis, K., Karion, A., Moser, B., and Richardson, S.: Quan-

tification and source apportionment of the methane emission flux from the city of Indianapolis, Elementa: Science of the Anthropocene, 3, 000 037, https://doi.org/10.12952/journal.elementa.000037, 2015.

O'Shea, S. J., Allen, G., Fleming, Z. L., Bauguitte, S. J., Percival, C. J., Gallagher, M. W., Lee, J., Helfter, C., and Nemitz, E.: Area fluxes of carbon dioxide, methane, and carbon monoxide derived from airborne measurements around Greater London: A case study during summer 2012, Journal of Geophysical Research: Atmospheres, 119, 4940–4952, https://doi.org/10.1002/2013JD021269, https://agupubs.onlinelibrary.wiley.com/doi/abs/10.1002/2013JD021269, 2013.

Peischl, J., Karion, A., Sweeney, C., Kort, E. A., Smith, M. L., Brandt, A. R., Yeskoo, T., Aikin, K. C., Conley, S. A., Gvakharia, A., Trainer, M., Wolter, S., and Ryerson, T. B.: Quantifying atmospheric methane emissions from oil and natural gas production in the Bakken shale region of North Dakota, Journal of Geophysical Research: Atmospheres, 121, 6101–6111, https://doi.org/10.1002/2015JD024631, https://agupubs.onlinelibrary.wiley.com/doi/abs/10.1002/2015JD024631, 2015.

Pitt, J. R., Le Breton, M., Allen, G., Percival, C. J., Gallagher, M. W., Bauguitte, S. J.-B., O'Shea, S. J., Muller, J. B. A., Zahniser, M. S., Pyle, J., and Palmer, P. I.: The development and evaluation of airborne in situ N_2O and CH_4 sampling using a quantum cascade laser absorption

spectrometer (QCLAS), Atmospheric Measurement Techniques, 9, 63–77, https://doi.org/10.5194/amt-9-63-2016, https://www.atmos-meas-tech.net/9/63/2016/, 2016.

Ravishankara, A. R., Daniel, J. S., and Portmann, R. W.: Nitrous Oxide (N2O): The Dominant Ozone-Depleting Substance Emitted in the 21st Century, Science, 326, 123–125, https://doi.org/10.1126/science.1176985, http://science.sciencemag.org/content/326/5949/123, 2009.

Richter, D., Weibring, P., Walega, J. G., Fried, A., Spuler, S. M., and Taubman, M. S.: Compact highly sensitive multi-species airborne mid-IR spectrometer, Applied Physics B, 119, 119–131, https://doi.org/10.1007/s00340-015-6038-8, https://doi.org/10.1007/s00340-015-6038-8, 2015.

Rothman, L. S., Gordon, I. E., Babikov, Y., Barbe, A., Chris Benner, D., Bernath, P. F., Birk, M., Bizzocchi, L., Boudon, V., Brown, L. R., Campargue, A., Chance, K., Cohen, E. A., Coudert, L. H., Devi, V. M., Drouin, B. J., Fayt, A., Flaud, J.-M., Gamache, R. R., Harrison, J. J., Hartmann, J.-M., Hill, C., Hodges, J. T., Jacquemart, D., Jolly, A., Lamouroux, J., Le Roy, R. J., Li, G., Long, D. A., Lyulin, O. M., Mackie, C. J., Massie, S. T., Mikhailenko, S., Müller, H. S. P., Naumenko, O. V., Nikitin, A. V., Orphal, J., Perevalov, V., Perrin, A., Polovtseva, E. R., Richard, C., Smith, M. A. H., Starikova, E., Sung, K., Tashkun, S., Tennyson, J., Toon, G. C., Tyuterev, V. G., and Wagner, G.: The HITRAN2012 molecular spectroscopic database, jqsrt, 130, 4–50, https://doi.org/10.1016/j.jqsrt.2013.07.002, 2013.

Santoni, G. W., Daube, B. C., Kort, E. A., Jiménez, R., Park, S., Pittman, J. V., Gottlieb, E., Xiang, B., Zahniser, M. S., Nelson, D. D., McManus, J. B., Peischl, J., Ryerson, T. B., Holloway, J. S., Andrews, A. E., Sweeney, C., Hall, B., Hintsa, E. J., Moore, F. L., Elkins, J. W., Hurst, D. F., Stephens, B. B., Bent, J., and Wofsy, S. C.: Evaluation of the airborne quantum cascade laser spectrometer (QCLS) measurements of the carbon and greenhouse gas suite CO_2, CH_4, N_2O, and CO during the CalNex and HIPPO campaigns, Atmospheric Measurement Techniques, 7, 1509–1526, https://doi.org/10.5194/amt-7-1509-2014, https://www.atmos-meas-tech.net/7/1509/2014/, 2014.

Simpson, I. J., Sulbaek Andersen, M. P., Meinardi, S., Bruhwiler, L., Blake, N. J., Helmig, D., Rowland, F. S., and Blake, D. R.: Long-term decline of global atmospheric ethane concentrations and implications for methane, Nature, 488, 490 EP –, http://dx.doi.org/10.1038/nature11342, 2012.

Smith, M. L., Kort, E. A., Karion, A., Sweeney, C., Herndon, S. C., and Yacovitch, T. I.: Airborne Ethane Observations in the Barnett Shale: Quantification of Ethane Flux and Attribution of Methane Emissions, Environmental Science & Technology, 49, 8158–8166, https://doi.org/10.1021/acs.est.5b00219, https://doi.org/10.1021/acs.est.5b00219, pMID: 26148554, 2015.

Vurgaftman, I., Weih, R., Kamp, M., Meyer, J. R., Canedy, C. L., Kim, C. S., Kim, M., Bewley, W. W., Merritt, C. D., Abell, J., and Höfling, S.: Interband cascade lasers, Journal of Physics D: Applied Physics, 48, 123 001, http://stacks.iop.org/0022-3727/48/i=12/a=123001, 2015.

Zellweger, C., Emmenegger, L., Firdaus, M., Hatakka, J., Heimann, M., Kozlova, E., Spain, T. G., Steinbacher, M., van der Schoot, M. V., and Buchmann, B.: Assessment of recent advances in measurement techniques for atmospheric carbon dioxide and methane observations, Atmospheric Measurement Techniques, 9, 4737–4757, https://doi.org/10.5194/amt-9-4737-2016, https://www.atmos-meas-tech.net/9/4737/2016/, 2016.

Zhao, C. L. and Tans, P. P.: Estimating uncertainty of the WMO mole fraction scale for carbon dioxide in air, Journal of Geophysical Research: Atmospheres, 111, https://doi.org/10.1029/2005JD006003, https://agupubs.onlinelibrary.wiley.com/doi/abs/10.1029/2005JD006003, 2006.